A Unified Approach to Optimizing Performance in Networks Serving Heterogeneous Flows

Ruogu Li, *Student Member, IEEE*, Atilla Eryilmaz, *Member, IEEE*, Lei Ying, *Member, IEEE*, and Ness B. Shroff, *Fellow, IEEE*

***Abstract*—We study the optimal control of communication networks in the presence of heterogeneous traffic requirements. Specifically, we distinguish the flows into two crucial classes: *inelastic* for modeling high-priority, delay-sensitive, and fixed-throughput applications; and *elastic* for modeling low-priority, delay-tolerant, and throughput-greedy applications. We note that the coexistence of such diverse flows creates complex interactions at multiple levels (e.g., flow and packet levels), which prevent the use of earlier design approaches that dominantly assume homogeneous traffic. In this work, we develop the mathematical framework and novel design methodologies needed to support such heterogeneous requirements and propose provably optimal network algorithms that account for the multilevel interactions between the flows. To that end, we first formulate a network optimization problem that incorporates the above throughput and service prioritization requirements of the two traffic types. We, then develop a distributed joint load-balancing and congestion control algorithm that achieves the dual goal of maximizing the aggregate utility gained by the elastic flows while satisfying the fixed throughput and prioritization requirements of the inelastic flows. Next, we extend our joint algorithm in two ways to further improve its performance: in delay through a virtual queue implementation with minimal throughput degradation and in utilization by allowing for dynamic multipath routing for elastic flows. A unique characteristic of our proposed dynamic routing solution is the novel two-stage queueing architecture it introduces to satisfy the service prioritization requirement.**

***Index Terms*—*[Author, please supply index terms/keywords for your paper. To download the IEEE Taxonomy go to http://www.ieee.org/documents/2009Taxonomy_v101.pdf]*.

I. Introduction

OVER the last several years, we have witnessed the development of increasingly sophisticated optimization and control techniques to address a variety of resource allocation problems for communication networks (e.g., [1], [2], [6], [7], [11], [12], [14], [16], [19], [21], [24], and [27]; see [9] and [18] for an overview). Much of this investigation has focused primarily on optimizing functions of long-term performance metrics such as throughput subject to network stability. Two types of traffic can be distinguished: elastic traffic with controllable packet injection rates generated by file transfer or other delay-tolerant applications, and inelastic traffic with fixed packet injection rates generated by delay-sensitive applications. Much of the existing work focuses on the existence of either the inelastic (e.g., [8], [22], and [28]) or the elastic (e.g., [6], [7], [12], [17], and [21]) traffic alone. The integration of elastic and inelastic flows in single-hop wireless systems has been studied in [3], [23], and [25] and has been extended to a multiple-hop network in [10], [14], and [27], however with the restriction of every flow having a single route. In [27], the coexistence of inelastic and elastic flows has also been considered in a more general setup.

However, previous utility maximization-based solutions do not distinguish inelastic packets and elastic packets at the packet level. Thus, the inelastic packets need to compete with elastic packets for link bandwidths, so these two types of flows have comparable delay performance. Yet, inelastic flows model delay-sensitive traffic and must be served with higher priority as they traverse the network. Our framework differs from earlier utility maximization-based approaches in that we give strictly higher service priority to inelastic packets, i.e., at every link, elastic packets can be transmitted only when there are no inelastic packets waiting for service. This prioritization decouples the inelastic packets and elastic packets at the *link (or, equivalently, packet) level* and will result in small delays for inelastic flows. Note that even though two types of flows are decoupled at the link level, to provide high utilization for elastic traffic, the inelastic flows must smartly distribute their load among their available routes. To that end, we developed our algorithm to maximize the network utility defined by elastic flows under the prioritization, which provides new coupling methods at the *flow level* that are different from previous utility maximization-based solutions.

We believe the main contributions of this work to be the following.

- The mathematical formulation of the utility maximization problem for elastic rate control subject to inelastic traffic requirements of fixed rate and service prioritization.
- The development of a distributed joint load-balancing and rate-control algorithm that gives strict service priority to inelastic packets while guaranteeing optimal resource utilization for elastic traffic. The description and the opti-

Manuscript received September 07, 2009; revised March 22, 2010 and June 11, 2010; accepted June 24, 2010; approved by IEEE/ACM TRANSACTIONS ON NETWORKING Editor E. Modiano. This work was supported in part by DTRA Grants HDTRA1-08-1-0016 and HDTRA1-09-1-0055, ARO MURI Award W911NF-08-1-0238, and NSF Awards 0626703-CNS, 0635202-CCF, 0721236-CNS, 08-31756, 09-53165, 953515-CNS, and 0916664-CCF. An earlier version of this work appeared in the *Proceedings of IEEE INFOCOM*, April 2009.

R. Li, A. Eryilmaz, and N. B. Shroff are with the Department of Electrical and Computer Engineering, The Ohio State University, Columbus, OH 43210 USA (e-mail: lir@ece.osu.edu; eryilmaz@ece.osu.edu; shroff@ece.osu.edu).

L. Ying is with the Department of Electrical and Computer Engineering, Iowa State University, Ames, IA 50010 USA (e-mail: leiying@engineering.iastate.edu).

Color versions of one or more of the figures in this paper are available online at http://ieeexplore.ieee.org.

Digital Object Identifier 10.1109/TNET.2010.2059038

1063-6692/$26.00 © 2010 IEEE

IEEE Proof Version

mality of this algorithm are provided for both the fluid model and the actual stochastic network.
- The extension of the base algorithm to a virtual queue-based operation that enables further delay reduction for both traffic types with a nominal and controllable sacrifice in the network utilization.
- The relaxation of the static route assumption for the elastic flows to achieve higher utilization of the network resources through dynamic, multipath routing while maintaining the prioritization requirements. This leads to a novel two-stage queueing architecture that complies with the prioritization requirements of the design.

The rest of the paper is organized as follows. We introduce our system model and formulate the main stochastic network optimization problem in Section II. In Section III, we first analyze a simple fluid version of the problem, and then using the insights gained to extend the solution to the stochastic scenario. In Section IV, we extend the algorithm in two practically important directions that improve delay performance and allow for dynamic multipath routing for elastic traffic. The simulation results and our concluding remarks are provided in Sections V and VI, respectively.

II. System Model and Objectives

We consider a fixed network represented by a graph $\mathcal{G} = (\mathcal{N}, \mathcal{L})$, where $\mathcal{N}$ is the set of nodes and $\mathcal{L}$ is the set of directed links. We assume that the capacity of link $l \in \mathcal{L}$ is c_l, and define the vector of link capacities as $\mathbf{c} := (c_l)_{l\in\mathcal{L}}$. Time is slotted in our system, and the external packets arrive at the beginning of each time slot.

We consider the scenario where the network resources are shared by a set of *inelastic* and *elastic flows*, where a flow is defined by its source node and destination node. While the inelastic flow represents traffic with fixed rates and stringent delay constraints such as voice and video streaming, the elastic flow represents delay-tolerant traffic with adaptive rates such as non-real-time file sharing and e-mail applications. The set of all flows in the network is denoted by $\mathcal{F}$, which is partitioned into two subsets, $\mathcal{F}_e$ and $\mathcal{F}_i$, where $\mathcal{F}_\mathrm{e}$ is the set of elastic flows and $\mathcal{F}_\mathrm{i}$ is the set of inelastic flows. Next, we describe the characteristics of inelastic and elastic flows in more detail.

Inelastic Flow: We let f_i denote an inelastic flow in the network with source s_i and destination d_i. Each inelastic flow f_i is associated with a fixed set of routes $\mathcal{R}_\mathrm{i}$. The rth route of this set is described by a vector $\mathbf{R}_\mathrm{i}^{(r)}$ such that $\mathbf{R}_\mathrm{i}^{(r)}[l] = 1$ if link $l \in \mathcal{L}$ is on that route, and zero otherwise. Let $x_\mathrm{i}^{(r)}[t]$ be the number of injected packets on the rth route of flow f_i at time slot t, and let $\mathbf{x}_\mathrm{i}[t] := \left(x_\mathrm{i}^{(r)}[t]\right)_{f_\mathrm{i}\in\mathcal{F}_\mathrm{i}}^{\mathbf{R}^{(r)}\in\mathcal{R}_\mathrm{i}}$ be the vector of inelastic flow packets injected on each route in slot t. Note that we slightly abuse our notation by using $\mathbf{x}_\mathrm{i}$ to denote rate vector of all inelastic flows, while $x_\mathrm{i}^{(r)}$ stands for the rate of flow $f_\mathrm{i} \in \mathcal{F}_\mathrm{i}$ over route $r \in \mathcal{R}_\mathrm{i}$. We assume that the packet arrivals of the inelastic flow f_i follow a stochastic process $A_\mathrm{i}[t]$ that is identically and independently distributed (*i.i.d.*) over time with a fixed mean rate, denoted by $a_\mathrm{i} := \mathbb{E}(A_\mathrm{i}[t])$, and a finite second moment, i.e., $\mathbb{E}\left(A_\mathrm{i}^2[t]\right) < \infty$.

To clarify the difference between $A_\mathrm{i}[t]$ and $\left(x_\mathrm{i}^{(r)}[t]\right)_{r\in\mathcal{R}_\mathrm{i}}$, we note that $A_\mathrm{i}[t]$ denotes the number of packets *generated* by flow f_i while $\left(x_\mathrm{i}^{(r)}[t]\right)_{r\in\mathcal{R}_\mathrm{i}}$ describes the number of packets *injected* into the network to traverse each of the available routes of flow f_i. Thus, $A_\mathrm{i}[t]$ is an uncontrollable stochastic process describing exogenous arrivals, whereas $\left(x_\mathrm{i}^{(r)}[t]\right)_{r\in\mathcal{R}_\mathrm{i}}$ is controllable by the network algorithm.

For notational convenience, we define

$$z_l(\mathbf{x}_\mathrm{i}[t]) := \sum_{f_\mathrm{i}\in\mathcal{F}_\mathrm{i}} \sum_{r=1}^{|\mathcal{R}_\mathrm{i}|} x_\mathrm{i}^{(r)}[t]\mathbf{R}_\mathrm{i}^{(r)}[l]$$

to denote the total number of inelastic packets on link l for a given $\mathbf{x}_\mathrm{i}[t]$.

Elastic Flow: We let f_e denote an elastic flow in the network with source s_e and destination d_e. In Section IV-B, we will consider dynamic routing for the elastic flow, but for now we will concentrate on the fix route case to get some insight about the load balancing. Here, we assume that each elastic flow f_e is associated with a single route $\mathbf{R}_\mathrm{e}$, and we let $x_\mathrm{e}[t]$ be the number of injected packets of flow f_e in slot t. Similar to the inelastic case, we also define $\mathbf{x}_\mathrm{e}[t] := (x_\mathrm{e}[t])_{f_\mathrm{e}\in\mathcal{F}_\mathrm{e}}$ to be the vector of elastic flow rates in slot t, and

$$y_l(\mathbf{x}_\mathrm{e}[t]) := \sum_{f_\mathrm{e}\in\mathcal{F}_\mathrm{e}} x_\mathrm{e}[t]\mathbf{R}_\mathrm{e}[l]$$

to denote the total number of elastic packets on link l. Associated with each elastic flow f_e, there exists a utility function $U_\mathrm{e}(\cdot)$ that measures the "satisfaction" of that flow as a function of its mean injection rate $\bar{x}_\mathrm{e} := \lim_{T\to\infty} \frac{1}{T}\sum_{t=0}^{T-1} x_\mathrm{e}[t]$. We also assume that the sources of the elastic flows are always infinitely backlogged.[1]

In the text, we use $\mathbf{x}[t] := (\mathbf{x}_\mathrm{i}[t], \mathbf{x}_\mathrm{e}[t])$ to denote the vector of inelastic and elastic packets injected into the network in slot t. Next, we provide a set of assumptions to be used later in the analysis.

Assumption 1: The elastic routing matrix $[\mathbf{R}_\mathrm{e}]_{f_\mathrm{e}\in\mathcal{F}_\mathrm{e}}$ has full row rank, which guarantees that given $\mathbf{q}$, there exists a unique $\mathbf{p}$ such that $\mathbf{q} = ([\mathbf{R}_\mathrm{e}]_{f_\mathrm{e}\in\mathcal{F}_\mathrm{e}})^T\mathbf{p}$.

Assumption 2: The inelastic arrival process $\{A_\mathrm{i}[t]\}_{f_\mathrm{i}\in\mathcal{F}_\mathrm{i}}$ is such that there exists a vector $\mathbf{x}_\mathrm{i}$ satisfying

$$\sum_{r=1}^{|\mathcal{R}_\mathrm{i}|} x_\mathrm{i}^{(r)} = a_\mathrm{i} \forall\ f_\mathrm{i} \in \mathcal{F}_\mathrm{i} \quad \text{and} \quad z_l(\mathbf{x}_\mathrm{i}) < c_l \forall\ l \in \mathcal{L}.$$

This condition implies that the inelastic flows are supportable by the network, i.e., there exists a rate division of the inelastic flow rates over their available routes that can support the arriving traffic.

Assumption 3: The utility functions $\{U_\mathrm{e}(x_\mathrm{e})\}_{f_\mathrm{e}}$ are strictly concave, twice differentiable, and increasing functions. Such an assumption is commonly used to capture the diminishing returns to the elastic flows of an increase in the service rate.

[1]We note that the rate controller with source reservoir as in [21] that considers arbitrary load scenario can be added on top of our algorithm.

IEEE Proof Web Version

Assumption 4: For each elastic flow $f_{\rm e} \in \mathcal{F}_{\rm e}$, its utility function $U_{\rm e}(x)$ satisfies the following: For each $m > 0$ and $M \in [m, \infty)$, there exists $\tilde{c}_1$, $\tilde{C}_1$, $\tilde{c}_2$, and $\tilde{C}_2$, with $0 < \tilde{c}_1 < \tilde{C}_1 < +\infty, 0 < \tilde{c}_2 < \tilde{C}_2 < +\infty$, satisfying $\tilde{c}_1 \leq U''_{\rm e}(x) \leq \tilde{C}_1$, $\tilde{c}_2 \leq \left(U'^{-1}_{\rm e}\right)'(x) \leq \tilde{C}_2$, for all $x \in [m, M]$.

We note that Assumption 1 is not critical in the proof of stability, but will simplify our proof, and we will eventually relax the single-route constraint on the elastic flows in Section IV-B. Also note that Assumptions 3 and 4 on the utility functions are not restrictive and hold for the following class of utility functions $U(x) = w > x^{(1-a)}/(1-a)$, for $a > 0$, which is known to characterize a large class of fairness concepts such as max-min fairness and weighted-proportional fairness (see [26] and the references therein).

In subsequent discussions, when the distinction between real and nonreal-time routes is unnecessary, we will simply refer to a route as $\mathbf{R}$ without any subscripts. Furthermore, for simplicity, we will use $z_l[t]$ for $z_l(\mathbf{x}_{\rm i}[t])$ and $y_l[t]$ for $y_l(\mathbf{x}_{\rm e}[t])$.

Queueing Architecture and Evolution: In our system, for each link $(i,j) \in \mathcal{L}$, a single-priority queue is maintained at the transmitting node i, which holds all the packets whose routes traverse (i,j). Since the inelastic flows are expected to have more stringent delay constraints, their packets are always stored ahead of those of the elastic flows, giving inelastic traffic full priority over its elastic counterpart. We let $p_l[t]$ denote the queue length of the buffer associated with link l at the beginning of slot t, and define

$$q_{\mathbf{R}}[t] = \sum_{l \in \mathcal{L}} \mathbf{R}[l] p_l[t]$$

to be the total queue length on route $\mathbf{R}$. Notice that $p_l[t]$ and $q_{\mathbf{R}}[t]$ counts both the inelastic and elastic flows' packets.

During each time slot, the queue p_l evolves as

$$p_l[t+1] = (p_l[t] + y_l[t] + z_l[t] - c_l)^+ \tag{1}$$

where $x^+ = \max(0, x)$. This evolution is based on a *link-centric* decomposition ([18]) and implicitly assumes that packets injected into the source nodes by the flows, denoted by $\mathbf{x}[t]$, arrive at the downstream nodes instantaneously. In reality, packets will reach downstream nodes only after a queueing and propagation delay incurred in the intermediate nodes. It is shown in prior works [5], [18], [29], [30] that the inclusion of these dynamics does not affect the long-term stability and fairness characteristics of the system. In particular, a *regulator* queue for each flow can be added to our queueing architecture before the queues associated with each link as the same architecture in [5]. The prioritization in the per-link queue does not affect the queue evolution, hence the results in [5] apply in our model with priority. Thus, in this work we use the evolution in (1), which possesses a more tractable and cleaner form.

Definition 1 (Stability): We say that a queue $q_{\mathbf{R}}$ is *stable* if

$$\limsup_{T \to \infty} \frac{1}{T} \sum_{t=0}^{T-1} \mathbb{E}(q_{\mathbf{R}}[t]) \leq B \tag{2}$$

where B is some finite positive value. We say that the *network is stable* if all aggregate queues $\{q_{\mathbf{R}}\}$ for both inelastic and elastic flows are stable.

Given this network and traffic model, we aim to do the following.

- Develop a mechanism that maximizes the total utility achieved by elastic flows while giving strict priority to and satisfying the rate demands of the inelastic traffic. To that end, we design a joint congestion control and load-balancing algorithm in Section III.
- Investigate means of extending our mechanism to improve the delay performance of both types of flows. To that end, we extend our joint algorithm in Section IV-A by adding appropriately constructed virtual queues with controllable parameters into the framework to achieve delay improvements.
- By relaxing the single-route constraint (and thus removing Assumption 1) on the elastic flow and adapting a new queueing architecture, we develop a joint congestion control, dynamic routing, and load-balancing algorithm in Section IV-B.

Before addressing these goals, we note that the load-balancing component of our joint algorithm will dynamically control the distribution the inelastic flow rates over its available routes. Thus, the effect of inelastic traffic on the elastic traffic cannot be simply modeled as a constant decrease in the capacity of the network, and a more sophisticated approach is needed. In particular, the inelastic flow rates on each route must be balanced optimally to allow for the maximum utilization of the network resources by the competing elastic flows. We develop such an algorithm in Section III.

III. Joint Congestion Control and Load Balancing

In this section, we address our first main objective, i.e., that of developing an algorithm that provides maximum utilization of elastic traffic while guaranteeing the support of inelastic traffic. We start by describing our objective mathematically in the form of a stochastic optimization problem.

Stochastic Network Optimization (SNO) Problem:

$$\begin{aligned} \max_{\{\mathbf{x}[t] \geq 0\}_{t \geq 0}} \quad & \sum_{f_{\rm e} \in \mathcal{F}_{\rm e}} U_{\rm e}(\bar{x}_{\rm e}) \\ s.t. \quad & \text{Queue Evolution as in } (1) \\ & \text{Network Stability as in } (2) \\ & \sum_{r=1}^{|\mathcal{R}_{\rm i}|} x_{\rm i}^{(r)}[t] = A_{\rm i}[t] \qquad \forall\, f_{\rm i} \in \mathcal{F}_{\rm i} \quad \forall\, t > 0. \end{aligned} \tag{3}$$

We solve this problem by first analyzing a simpler deterministic fluid model in Section III-A. The solution to this fluid model will help in exposition as well as in providing insights on the solution of the above more complex problem. Then, we return in Section III-B to the stochastic problem.

A. Heuristic Fluid Model

In the fluid model scenario, all the dynamics and randomness are ignored, and the stochastic constraints are replaced with static constraints. In particular, the inelastic flow $f_{\rm i}$ is assumed to have a fixed arrival rate $a_{\rm i}$, and the network stability condition is replaced by a condition on total link rate being no more

IEEE Proof Web Version

than capacity. Then, the SNO problem reduces to the following problem in this scenario.

Fluid Network Optimization (FNO) Problem:

$$\max_{\mathbf{x}\geq 0} \quad \sum_{f_\mathrm{e}\in\mathcal{F}_\mathrm{e}} U_\mathrm{e}(x_\mathrm{e})$$
$$s.t. \quad y_l(\mathbf{x}_\mathrm{e}) + z_l(\mathbf{x}_\mathrm{i}) \leq c_l \qquad \forall\, l\in\mathcal{L} \tag{4}$$
$$\sum_{r=1}^{|\mathcal{R}_\mathrm{i}|} x_\mathrm{i}^{(r)} = a_\mathrm{i} \qquad \forall\, f_\mathrm{i}\in\mathcal{F}_\mathrm{i}. \tag{5}$$

In our discussion, we will abbreviate the aggregate elastic and inelastic rates, $y_l(\mathbf{x}_\mathrm{e})$ and $z_l(\mathbf{x}_\mathrm{i})$, with y_l and z_l for brevity. We note that condition (4) aims to capture the network stability condition in the fluid model by guaranteeing that the total load on a link is below the link capacity, and condition (5) guarantees that inelastic flows receive enough bandwidth to satisfy its rate demands. Thus, the optimization problem is to maximize the sum of utilities of elastic flows when guaranteeing that inelastic flows are supported.

It is not difficult to show that the optimum value of FNO is an upper bound for the optimum value of SNO. To see this, note that any solution $\{\mathbf{x}[t]\}_{t\geq 0}$ that solves SNO must also satisfy $\bar{y}_l + \bar{z}_l \leq c_l$, where $\bar{y}_l := \lim_{T\to\infty}\frac{1}{T}\sum_{t=0}^{T-1} y_l(\mathbf{x}[t])$, and $\bar{z}_l$ is defined similarly. Otherwise, the queue l cannot be stable. This is equivalent to condition (4) in FNO. Thus, FNO contains all the feasible points of SNO. In Section III-B, we will design an algorithm under which SNO can get arbitrarily close to the FNO solution, and thus guarantees the optimality of SNO.

We start by showing that there exists a unique $\mathbf{x}_\mathrm{e} = \{x_\mathrm{e}\}_{f_\mathrm{e}\in\mathcal{F}_\mathrm{e}}$ that solves the FNO problem under Assumptions 2 and 3.[2]

Proposition 1: If Assumptions 2 and 3 hold, then the $\mathbf{x}_\mathrm{e}^* = \{x_\mathrm{e}\}_{f_\mathrm{e}\in\mathcal{F}_\mathrm{e}}$ that solves the network optimization problem is unique.

Proof: The optimization problem has a unique solution because the utility functions are strictly concave, and constraints (4) and (5) are linear. ∎

To solve the FNO problem, we construct a partial Lagrangian. Define α_l to be the Lagrange multipliers associated with constraint (4). Then, the partial Lagrangian can be written as

$$\begin{aligned} L(\mathbf{x}_\mathrm{i},\mathbf{x}_\mathrm{e},\alpha) &= \sum_{f_\mathrm{e}\in\mathcal{F}_\mathrm{e}} U_\mathrm{e}(x_\mathrm{e}) - \sum_{l\in\mathcal{L}}\alpha_l(z_l + y_l - c_l) \\ &= \sum_{f_\mathrm{e}\in\mathcal{F}_\mathrm{e}}\left(U_\mathrm{e}(x_\mathrm{e}) - \left(\sum_{l:\mathbf{R}_\mathrm{e}^{(r)}[l]=1}\alpha_l\right)x_\mathrm{e}\right) \\ &\quad + \sum_{l\in\mathcal{L}}\alpha_l(c_l - z_l). \end{aligned}$$

Since the FNO problem satisfies Slater's condition [4] due to Assumption 2, the strong duality holds. We can then conclude that there exists $\mathbf{x}^* := (\mathbf{x}_\mathrm{e}^*, \mathbf{x}_\mathrm{i}^*)$, and $\alpha^* := (\alpha_l)_l$ such that:

- $\mathbf{x}^*$ solves the FNO problem;
- $\mathbf{x}^* \in \arg\max_{\mathbf{x}\geq 0} L(\mathbf{x}_\mathrm{i}, \mathbf{x}_\mathrm{e}, \alpha^*)$.

[2]We note that the strict concavity assumption in Assumption 3 can be relaxed, and our results can be extended to state that the elastic rates converge to the *set* of optimal rates rather than the *unique* optimum rate.

Note that

$$\begin{aligned} \max L(\mathbf{x},\alpha^*) = \max &\sum_{f_\mathrm{e}\in\mathcal{F}_\mathrm{e}}\left(U_\mathrm{e}(x_\mathrm{e}) - \beta^*_{\mathbf{R}_\mathrm{e}} x_\mathrm{e}\right) \\ &- \min\sum_{l\in\mathcal{L}}\alpha_l^* z_l + \sum_{l\in\mathcal{L}}\alpha_l^* c_l \end{aligned}$$

where $\beta_{\mathbf{R}} := \sum_{l\in\mathcal{L}}\mathbf{R}[l]\alpha_l$. This decomposition suggests the following conditions.

(i) The elastic flow f_e should allocate its rates such that

$$x_\mathrm{e}^* = U_\mathrm{e}'^{-1}\left(\beta^*_{\mathbf{R}_\mathrm{e}}\right). \tag{6}$$

(ii) The inelastic flow f_i should distribute its packets over its available routes $\left\{x_\mathrm{i}^{*(r)}\right\}_{r\in\mathcal{R}_\mathrm{i}}$ such that

$$\begin{aligned} \min \quad & \sum_{r=1}^{|\mathcal{R}_\mathrm{i}|} x_\mathrm{i}^{(r)}\beta^*_{\mathbf{R}_\mathrm{i}^{(r)}} \\ s.t. \quad & \sum x_\mathrm{i}^{(r)} = a_\mathrm{i}. \end{aligned} \tag{7}$$

Since the optimization problem (7) has a linear objective, the following lemma holds [4].

Lemma 1: For any $\mathbf{R}_\mathrm{i}^{(r)} \in \mathcal{R}_\mathrm{i}$, we have:

- $\beta^*_{\mathbf{R}_\mathrm{i}^{(r)}} = \beta^*_{\mathbf{R}_\mathrm{i}^{(r')}}$ if $x_\mathrm{i}^{*(r)} > 0$ and $x_\mathrm{i}^{*(r')} > 0$;
- $\beta^*_{\mathbf{R}_\mathrm{i}^{(r)}} < \beta^*_{\mathbf{R}_\mathrm{i}^{(r')}}$ if $x_\mathrm{i}^{*(r)} > 0$ and $x_\mathrm{i}^{*(r')} = 0$.

This lemma implies that considering an inelastic flow f_i, all routes in the optimal solution with a positive flow have the same value of β.

We note that α_l of FNO is closely associated with the queue length p_l of SNO, and correspondingly $\beta_{\mathbf{R}}$ of FNO is closely associated with the aggregate queue length on a route $q_{\mathbf{R}}$ of SNO. Such connections are revealed and exploited in several earlier works for designing different network algorithms (e.g., [6], [7], [16], [17], and [27]). The following algorithm is a continuous-time version of the Lagrangian method for finding the optimum solution of FNO. This algorithm will later be used to solve the SNO. To distinguish the continuous-time evolution from the discrete-time evolution, we use (t) to denote continuous-time index, while $[t]$ denotes discrete-time index.

Joint Congestion Control and Load-Balancing Algorithm for the FNO Problem:

- Queue evolution for link l

$$\dot{p}_l(t) := \frac{dp(t)}{dt} = (z_l(t) + y_l(t) - c_l)^+_{p_l(t)}$$

  where $(v(t))^+_{p(t)}$ is zero if $v(t) < 0$ and $p(t) = 0$; and $v(t)$ otherwise.
- Congestion controller for elastic flow f_e

$$x_\mathrm{e}(t) = U_\mathrm{e}'^{-1}(q_{\mathbf{R}_\mathrm{e}}(t)).$$

- Load balancing implemented for inelastic flow f_i

$$\dot{x}_\mathrm{i}^{(r)}(t) = \left(\bar{q}_\mathrm{i}(t) - q_{\mathbf{R}_\mathrm{i}^{(r)}}(t)\right)^+_{x_\mathrm{i}^{(r)}(t)} \tag{8}$$

IEEE Proof Version

where $\bar{q}_{\rm i}(t)$ satisfies

$$\sum_{r=1}^{|\mathcal{R}_{\rm i}|}\left(\bar{q}_{\rm i}(t)-q_{\mathbf{R}_{\rm i}^{(r)}}(t)\right)^{+}_{x_{\rm i}^{(r)}(t)}=0 \tag{9}$$

and $\sum_{r=1}^{|\mathcal{R}_{\rm i}|}x_{\rm i}^{(r)}(0)=a_{\rm i}$.

Remark: Note that the congestion control algorithm is motivated by equality (6). The load-balancing algorithm (8) is motivated by Lemma 1. In particular, for each inelastic flow $f_{\rm i}$, when the system reaches the equilibrium, we have $\dot{x}_{\rm i}^{(r)}(t)=0$ for all r. This implies that $q_{\mathbf{R}_{\rm i}^{(r)}}(t)=\bar{q}_{\rm i}(t)$ for $x_{\rm i}^{(r)}(t)>0$ and $q_{\mathbf{R}_{\rm i}^{(r)}}(t)\geq\bar{q}_{\rm i}$ for $x_{\rm i}^{(r)}(t)=0$. Thus, at the equilibrium point, $q_{\mathbf{R}_{\rm i}^{(r)}}(t)$ satisfies Lemma 1. Furthermore, from (9), it is easy to see that

$$\sum_{r=1}^{|\mathcal{R}_{\rm i}|}x_{\rm i}^{(r)}(t)=a_{\rm i},\qquad\text{for all } t. \tag{10}$$

The intuition behind the load-balancing algorithm described above is to shift the inelastic flows to less heavily loaded routes to allow for the maximum network utilization for elastic flows. In the algorithm, a source needs all the queue information along its route. However, as we mentioned in Section II, we can send queue information hop by hop and still achieve stability even if this information is delayed. Thus, this algorithm can be implemented fully distributed.

Next, we will show the stability and optimality of our joint congestion control and load-balancing algorithm.

Proposition 2: Under Assumptions 1–3, the joint congestion control and load-balancing algorithm is globally asymptotically stable, i.e., $\lim_{t\to\infty}(\mathbf{x}_{\rm e}(t),\mathbf{x}_{\rm i}(t),\mathbf{p}(t),\mathbf{q}(t))=(\mathbf{x}_{\rm e}^*,\mathbf{x}_{\rm i}^*,\alpha^*,\beta^*)$, where $(\mathbf{x}_{\rm e}^*,\mathbf{x}_{\rm i}^*,\alpha^*,\beta^*)$ is an optimal prime-dual solution to the FNO problem. Furthermore, (10) holds.

Proof: The proof is provided in Appendix A. ∎

B. Stochastic Model

We now return to the original SNO problem with a minor variation.

SNO Problem with Parameter *K* (SNO-K):

$$\begin{aligned}\max_{\{\mathbf{x}[t]\geq 0\}_{t\geq 0}}\quad & \sum_{f_{\rm e}\in\mathcal{F}_{\rm e}}KU_{\rm e}(\bar{x}_{\rm e})\\ s.t.\quad & \text{Queue Evolution as in (1)}\\ & \text{Network Stability as in (2)}\\ & \sum_{r=1}^{|\mathcal{R}_{\rm i}|}x_{\rm i}^{(r)}[t]=A_{\rm i}[t]\qquad\forall\, f_{\rm i}\in\mathcal{F}_{\rm i}\quad\forall\, t>0\end{aligned}$$

where K is a positive design parameter. We will see that K-parameter is critical in eliminating the effect of randomness in the stochastic system on the long-term performance. Note that the solution to the SNO-K problem is independent of the value of K, and its optimum solution is identical to the solution of the SNO problem.

Motivated by the analysis in the fluid model, we propose the following joint congestion control and load-balancing algorithm.

Joint Congestion Control and Load-Balancing Algorithm for the SNO-K Problem:

- Scheduling with Strict Prioritization:
  For each link $l\in\mathcal{L}$, we serve c_l packets from p_l, with strict priority to inelastic packets, which leads to the following queue evolution:
  $$p_l[t+1]=(p_l[t]+z_l[t]+y_l[t]-c_l)^{+}.$$
- Congestion controller for elastic flow $f_{\rm e}$
  $$x_{\rm e}[t]=\min\left\{M,U_{\rm e}'^{-1}\left(\frac{1}{K}q_{\mathbf{R}_{\rm e}}[t]\right)\right\}$$
  where M is a positive constant satisfies $M>2\max_{l\in\mathcal{L}}\{c_l\}$.
- Load balancing implemented for inelastic flow $f_{\rm i}$
  $$\triangle x_{\rm i}^{(r)}[t]=\left(\bar{q}_{\rm i}[t]-q_{\mathbf{R}_{\rm i}^{(r)}}[t]\right)^{+}_{x_{\rm i}^{(r)}[t+1]}$$
  or equivalently
  $$x_{\rm i}^{(r)}[t+1]=\left(x_{\rm i}^{(r)}[t]+\bar{q}_{\rm i}[t]-q_{\mathbf{R}_{\rm i}^{(r)}}[t]\right)^{+}$$
  where $\bar{q}_{\rm i}[t]$ satisfies
  $$\sum_{r=1}^{|\mathcal{R}_{\rm i}|}\left(\bar{q}_{\rm i}[t]-q_{\mathbf{R}_{\rm i}^{(r)}}[t]\right)^{+}_{x_{\rm i}^{(r)}[t+1]}=A_{\rm i}[t+1]-A_{\rm i}[t]$$
  and $\sum_{r=1}^{|\mathcal{R}_{\rm i}|}x_{\rm i}^{(r)}[0]=A_{\rm i}[0]$.

Remark: The factor $1/K$ in the congestion control equation comes from the factor K in the optimization problem. It can be interpreted as the aggressiveness factor of the elastic flow, as the congestion controller is inclined to inject more packets into the network with larger K. Also note that the load-balancing implementation is slightly different from the fluid model version to accommodate the randomness in the arrival processes for inelastic flows. The update is modified to ensure that $\sum_{r=1}^{|\mathcal{R}_{\rm i}|}x_{\rm i}^{(r)}[t]=A_{\rm i}[t]$ holds for all t.

The next proposition establishes the stability and optimality of the joint algorithm for the stochastic system.

Proposition 3: Under Assumptions 1–4, the joint congestion control and load-balancing algorithm stabilizes the system in the sense that the Markov chain $(\mathbf{p}[t],\mathbf{x}_{\rm i}[t])$ is positive recurrent with

$$\limsup_{T\to\infty}\frac{1}{T}\sum_{t=0}^{T-1}\mathbb{E}\left(\left\|\mathbf{q}_{\mathbf{R}_{\rm e}}[t]-\beta^*_{\mathbf{R}_{\rm e}}\right\|\right)\leq\frac{B+\epsilon\sigma K}{\epsilon}$$

and guarantees that the rate allocation satisfies

$$\limsup_{T\to\infty}\frac{1}{T}\sum_{t=0}^{T-1}\mathbb{E}\left(\|\mathbf{x}_{\rm e}[t]-\mathbf{x}_{\rm e}^*\|^2\right)\leq\frac{B}{\tilde{c}_3K}.$$

IEEE Proof Web Version

Here, $\mathbf{x}_{\mathrm{e}}^*$ is the optimal solution to the SNO-K problem, σ is an arbitrarily chosen positive constant, and ϵ and $\tilde{c}_3$ are positive values. ■

Proof: See [15] for the proof. ■

Note that as the design parameter K increases, the rate converges to the optimal allocation at the cost of increased equilibrium queue-length levels. While such tradeoffs between optimality and delay are observed in earlier works under a single type of traffic (e.g., [7] and [21]), in this work a new interaction is observed between inelastic and elastic traffic through the parameter K. In particular, larger values of K result in more aggressive elastic flows, resulting in larger queue lengths on the links they traverse. This forces the inelastic flows to redistribute their flows to less loaded routes. This increases the utilization of the network, while causing more delay to inelastic flows. In order to provide better delay performance to both types of traffic, in the next section we extend our base algorithm by using virtual queues.

IV. Extension of the Algorithm

In this section, we extend our joint congestion control and load-balancing algorithm in two important directions. We first provide a virtual queue-based solution that reduces the overall queue length with a negligible sacrifice in capacity. We then provide a solution that allows the dynamic routing for the elastic flow.

A. Virtual Queue Algorithm

Inelastic applications are delay-sensitive, hence we assume that packets from inelastic flows have strict priority over their elastic counterparts. Thus, the inelastic flows do not see the elastic flows in the queues they traverse. However, in some cases a link might be critically loaded by the inelastic traffic itself, thus resulting in large delays. Also, elastic traffic may have some delay constraints that are nonnegligible.

An effective way of reducing the experienced delay is by including virtual queues that are served at a fraction of the actual service rate and by using the virtual queue-length values as prices [13]. To that end, we introduce two types of virtual queues with parameters to the previous optimization problem, ρ_1 and ρ_2, which control the total load and the inelastic flow load, respectively.

Here for simplicity, we go back to the fluid model to design and analyze the joint congestion control and load-balancing algorithm using virtual queues. We would like to have $\tilde{\mathbf{x}}^* := (\tilde{\mathbf{x}}_{\mathrm{e}}^*, \tilde{\mathbf{x}}_{\mathrm{i}}^*)$ solve the following optimization problem.

FNO Problem With Virtual Queues (FNO-VQ):

$$\begin{aligned} \max_{\mathbf{x}\geq 0} \quad & \sum_{f_{\mathrm{e}}\in\mathcal{F}_{\mathrm{e}}} U_{\mathrm{e}}(x_{\mathrm{e}}) \\ s.t. \quad & y_l(\mathbf{x}_{\mathrm{e}}) + z_l(\mathbf{x}_{\mathrm{i}}) \leq \rho_1 c_l \qquad \forall\, l \in \mathcal{L} \\ & z_l(\mathbf{x}_{\mathrm{i}}) \leq \rho_2 c_l \qquad \forall\, l \in \mathcal{L} \\ & \sum_{r=1}^{|\mathcal{R}_{\mathrm{i}}|} x_{\mathrm{i}}^{(r)} = a_{\mathrm{i}} \end{aligned} \tag{11}$$

where $0 < \rho_2 \leq \rho_1 < 1$.

To guarantee the feasibility of this optimization problem, we replace our earlier Assumption 2 with Assumption 5.

Assumption 5: There exists an $\mathbf{x}_{\mathbf{i}}$ such that

$$\sum_{r=1}^{|\mathcal{R}_{\mathrm{i}}|} x_{\mathrm{i}}^{(r)} = a_{\mathrm{i}} \;\forall\, f_{\mathrm{i}} \in \mathcal{F}_{\mathrm{i}} \quad \text{and} \quad z_l(\mathbf{x}_{\mathbf{i}}) < \rho_2 c_l \;\forall\, l \in \mathcal{L}.$$

This can be viewed as admission control is done for the inelastic flow after we choose the parameter ρ_2 to ensure the feasibility of the problem.

To solve the FNO-VQ problem, we first introduce virtual queues for elastic and inelastic flows on each link, respectively. The virtual queue length $\theta_l(t)$ for elastic flows evolves as follows:

$$\dot{\theta}_l(t) = (z_l(t) + y_l(t) - \rho_1 c_l)^+_{\theta_l(t)}.$$

The virtual queue length for inelastic flows $\gamma_l(t)$ evolves as follows:

$$\dot{\gamma}_l(t) = (z_l(t) - \rho_2 c_l)^+_{\gamma_l(t)}.$$

Note that when the total instantaneous traffic load is larger than $\rho_1 c_l$ or the inelastic traffic load is larger than $\rho_2 c_l$, the virtual queues will build up, and the network controller will reduce the traffic load.

Based on this virtual queue scheme, we have the following joint congestion control and load-balancing algorithm.

Joint Congestion Control and Load-Balancing Algorithm for FNO-VQ Problem:

- Virtual queue evolution for a link l

$$\begin{aligned} \text{Elastic flows:} \quad & \dot{\theta}_l(t) = (z_l(t) + y_l(t) - \rho_1 c_l)^+_{\theta_l(t)} \\ \text{Inelastic flows:} \quad & \dot{\gamma}_l(t) = (z_l(t) - \rho_2 c_l)^+_{\gamma_l(t)}. \end{aligned}$$

- Congestion controller for elastic flow f_{e}

$$x_{\mathrm{e}}(t) = U_{\mathrm{e}}'^{-1}(s_{\mathbf{R}_{\mathrm{e}}}(t))$$

where $s_{\mathbf{R}_{\mathrm{e}}}(t) = \sum_{l:\mathbf{R}_{\mathrm{e}}[l]=1} \theta_l(t)$ is the aggregated virtual queue length of the elastic flow.

- Load balancing implemented for inelastic flow f_{i}

$$\dot{x}_{\mathrm{i}}^{(r)}(t) = \left(\bar{\mu}_{\mathrm{i}}(t) - \mu_{\mathbf{R}_{\mathrm{i}}^{(r)}}(t)\right)^+_{x_{\mathrm{i}}^{(r)}(t)}$$

where $\mu_{\mathbf{R}}(t) = \sum_{l:\mathbf{R}[l]=1}(\theta_l(t) + \gamma_l(t))$, $\bar{\mu}_{\mathrm{i}}(t)$ satisfies

$$\sum_{r=1}^{|\mathcal{R}_{\mathrm{i}}|} \left(\bar{\mu}_{\mathrm{i}}(t) - \mu_{\mathbf{R}_{\mathrm{i}}^{(r)}}(t)\right)^+_{x_{\mathrm{i}}^{(r)}(t)} = 0$$

and $\sum_{r=1}^{|\mathcal{R}_{\mathrm{i}}|} x_{\mathrm{i}}^{(r)}(0) = a_i$.

Remark: In the above algorithm, note that the congestion control algorithm only responds to the virtual queues for elastic flows, but the load-balancing algorithm responds to both the virtual queues for elastic flows and inelastic flows. Furthermore, the actual queue length is not used in the algorithm.

IEEE Proof Web Version

In the following proposition, we show the equilibrium point of the algorithm with virtual queue is the optimal solution of (11).

Proposition 4: Under Assumptions 1, 3, and 5, the virtual system under the joint congestion control and load-balancing algorithm for the FNO-VQ problem is globally asymptotically stable, i.e., $\lim_{t\to\infty}(\mathbf{x}_\mathrm{e}(t),\mathbf{x}_\mathrm{i}(t),\theta(t),\gamma(t)) = \left(\tilde{\mathbf{x}}_\mathrm{e}^*,\tilde{\mathbf{x}}_\mathrm{i}^*,\tilde{\theta}^*,\tilde{\gamma}^*\right)$, where $\left(\tilde{\mathbf{x}}_\mathrm{e}^*,\tilde{\mathbf{x}}_\mathrm{i}^*,\tilde{\theta}^*,\tilde{\gamma}^*\right)$ is an optimal primal-dual solution of the network optimization problem (11). ■

Proof: See [15] for the proof. ■

Remark: Proposition 4 implies the stability of the virtual system. Since the virtual system is run in a network with smaller link capacity, it is intuitively reasonable to expect the real queue lengths be stable. While this intuition is confirmed in numerical studies, we do not claim the stability of the real system under this algorithm.

The extension of this result to the stochastic scenario is omitted since it follows the same line of reasoning as in the joint congestion control and load-balancing algorithm of Section III.

B. Dynamic Routing for Elastic Flows

Here, we keep the assumptions of the inelastic flows and relax the single-route constraint on the elastic flows. Each elastic flow $f_\mathrm{e} = f_s^d$ now is associated with a source node $s \in \mathcal{N}$ and a destination node $d \in \mathcal{N}$. The injection rate of the flow f_s^d is denoted by x_s^d, and $U_s^d\left(x_s^d\right)$ is the utility function.

In this model, we adapt a new queueing architecture. Each node i maintains both real queues and virtual queues (counters), which are identical structural-wise. We focus on the virtual queues, which are neater to analyze.

Within the virtual queues, there are two levels of queues. The first level of the virtual queues are for each destination for elastic flows, denoted by $s_i^d[t]$, each node maintains $|\mathcal{N}|-1$ such queues. Let $r_{ij}^d[t]$ denote the promised service rate to elastic flows that are destined to d on link $l=(i,j)$, and let

$$y_l[t] = \sum_{d\in\mathcal{N}} r_{ij}^d[t]$$

denotes the total promised service of elastic flows on link l. These counters evolve as

$$s_i^d[t+1] = \left(s_i^d[t] + x_i^d[t] + \sum_{m\in\mathcal{N}} r_{mi}^d[t] - \sum_{j\in\mathcal{N}} r_{ij}^d[t]\right)^+. \tag{12}$$

The second level of virtual queues consists of a virtual queue for each outgoing link, denoted by $p_{ij}[t]$ where $(i,j)\in\mathcal{L}$, which counts packets from both inelastic and elastic flows. Packets of the inelastic flows are always "stored" ahead of those of the elastic flows. These counters evolve as

$$p_l[t+1] = (p_l[t] + y_l[t] + z_l[t] - c_l)^+. \tag{13}$$

Remark 1: Note that in the virtual queues (counters), $r_{ij}^d[t]$ virtual packets "bypass" the queueing in the second level of virtual queues and directly enter the corresponding first-level virtual queues of the next node, while $r_{ij}^d[t]$ actual packets are forwarded within the node to the second level of queues, waiting to be transmitted onto the corresponding link to the downstream node. The decisions made by the algorithm are based on the virtual queue information, which is a "prediction" of the actual queue lengths. We will see that the actual queues evolve in the same way when the system reaches its equilibrium point.

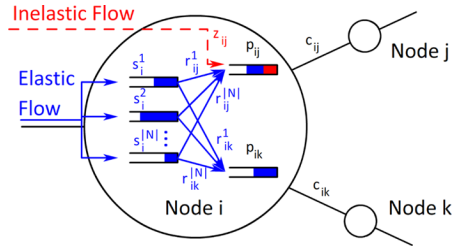

Fig. 1. Queueing architecture for dynamic routing.

Remark 2: The evolution of $p[t]$ given in (13) implicitly assumes that the inelastic packets injected into the source nodes arrive at the downstream nodes immediately. Prior works [5], [18], [29], [30] show that this assumption does not affect the long-term performance of the system. Since the inelastic traffic enters the second-level queues directly, the results of those works still apply to the inelastic flows. In particular, a regulator queue for each inelastic flow can be added to our queueing architecture before the second-level queues associated with each link following the same approach as in [5].

The queueing architecture described is illustrated in Fig. 1.

For simplicity, we consider the fluid model scenario for dynamic routing.

FNO Problem With Dynamic Routing (FNO-DR):

$$\max_{\mathbf{x}\geq 0} \quad \sum_{f_\mathrm{e}\in\mathcal{F}_\mathrm{e}} U_\mathrm{e}(x_\mathrm{e}) \tag{14}$$

$$s.t. \quad y_l(\mathbf{r}) + z_l(\mathbf{x}_\mathrm{i}) \leq c_l \qquad \forall\, l\in\mathcal{L} \tag{15}$$

$$\sum_{r=1}^{|\mathcal{R}_\mathrm{i}|} x_\mathrm{i}^{(r)} = a_\mathrm{i} \qquad \forall\, f_\mathrm{i}\in\mathcal{F}_\mathrm{i} \tag{16}$$

$$x_\mathrm{i}^d + \sum_{m\in\mathcal{N}} r_{mi}^d \leq \sum_{j\in\mathcal{N}} r_{ij}^d \qquad \forall\, i,d\in\mathcal{N}, i\neq d \tag{17}$$

$$r_{ij}^d \leq P \qquad \forall\,(i,j)\in\mathcal{L}, d\in\mathcal{N} \tag{18}$$

where (17) is the flow conservation constraint, and (18) is a fixed bound on r_{ij}^d, where $P \geq \max_{l\in\mathcal{L}}\{c_l\}$.

Based on the new queueing architecture and the FNO-DR problem, using the Lagrange multiplier approach, we have the following joint congestion control, dynamic routing, and load-balancing algorithm.

Joint Congestion Control, Dynamic Routing, and Load-Balancing Algorithm for the FNO-DR Problem:

- Virtual queue evolution

$$\dot{s}_i^d(t) = \left(x_i^d(t) + \sum_{m\in\mathcal{N}} r_{mi}^d(t) - \sum_{j\in\mathcal{N}} r_{ij}^d(t)\right)^+_{s_i^d(t)}$$

IEEE Proof Web Version

$$\dot{p}_l(t) = (z_l(t) + y_l(t) - c_l)^+_{p_l(t)}.$$

- Congestion controller for elastic flow f_s^d

$$x_s^d(t) = \left(U_s^d\right)'^{-1}\left(s_s^d(t)\right).$$

- Dynamic routing for elastic flow

$$\dot{r}_{ij}^d(t) = \begin{cases} s_i^d(t) - s_j^d(t) - p_{ij}(t), & \text{if } r_{ij}^d \in (0, P) \\ \left(s_i^d(t) - s_j^d(t) - p_{ij}(t)\right)^+, & \text{if } r_{ij}^d \le 0 \\ \left(s_i^d(t) - s_j^d(t) - p_{ij}(t)\right)^-, & \text{if } r_{ij}^d \ge P. \end{cases}$$

- Load balancing for inelastic flow f_{i}

$$\dot{x}_{\mathrm{i}}^{(r)}(t) = \left(\bar{q}_{\mathrm{i}}(t) - q_{\mathbf{R}_{\mathrm{i}}^{(r)}}(t)\right)^+_{x_{\mathrm{i}}^{(r)}(t)}$$

where $q_{\mathbf{R}_{\mathrm{i}}^{(r)}}(t) = \sum_{l\in\mathcal{L}} \mathbf{R}_{\mathrm{i}}[l] p_l(t)$, and $\bar{q}_{\mathrm{i}}(t)$ satisfies

$$\sum_{r=1}^{|\mathcal{R}_{\mathrm{i}}|} \left(\bar{q}_{\mathrm{i}}(t) - q_{\mathbf{R}_{\mathrm{i}}^{(r)}}(t)\right)^+_{x_{\mathrm{i}}^{(r)}(t)} = 0$$

and $\sum_{r=1}^{|\mathcal{R}_{\mathrm{i}}|} x_{\mathrm{i}}^{(r)}(0) = a_i$.

Remark: In the algorithm above, the rate control of the elastic traffic only needs the virtual queue information of the source node, while the load balancing of the inelastic uses the virtual queue information on the whole route. The dynamic routing algorithm for elastic traffic is similar to the back-pressure algorithm, while the backlog difference between the two nodes of a link $s_i^d - s_j^d$ is offset by p_{ij}, discouraging the elastic flows from using the links that are in the route of the inelastic flows. Also, we note that this back-pressure-like algorithm is applied to the elastic traffic only, and the strict priority of the inelastic traffic is still maintained.

In the following proposition, we show the equilibrium point of the algorithm for dynamic routing is the optimal solution of (14).

Proposition 5: Under Assumptions 2 and 3, the virtual system under the joint congestion control, dynamic routing, and load-balancing algorithm for the FNO-DR problem is globally asymptotically stable, i.e., $\lim_{t\to\infty}(\mathbf{x}_{\mathrm{e}}(t), \mathbf{x}_{\mathrm{i}}(t), \mathbf{p}(t), \mathbf{s}(t)) = (\hat{\mathbf{x}}_{\mathrm{e}}^*, \hat{\mathbf{x}}_{\mathrm{i}}^*, \hat{\mathbf{p}}^*, \hat{\mathbf{s}}^*)$ where $(\hat{\mathbf{x}}_{\mathrm{e}}^*, \hat{\mathbf{x}}_{\mathrm{i}}^*, \hat{\mathbf{p}}^*, \hat{\mathbf{s}}^*)$ is an optimal primal-dual solution of the network optimization problem (14).

Proof: The proof is provided in Appendix B. ■

Remark: Note that the virtual system will evolve to the optimal point according to the equations above, while the actual system may follow a slightly different trajectory. This is because during the transient period of evolution, the total incoming rate of inelastic flow $\mathbf{z}(t)$ and the elastic flow $\mathbf{r}(t)$ into the second level of the queue (cf. Fig. 1) is allowed to be larger than the capacity of the link. Thus, when the system made routing decisions according to the virtual values (the estimated number of packets in the queues), there may not be enough packets to transmit in the actual queues. However, when the virtual system converges to its equilibrium point, the assigned service rate r_{ij}^{*d} will be feasible as shown in Proposition 5, and therefore the actual system will also be able to provide the same rate as the virtual one. Thus, at the equilibrium point, the stability of the virtual system implies the stability of the actual system.

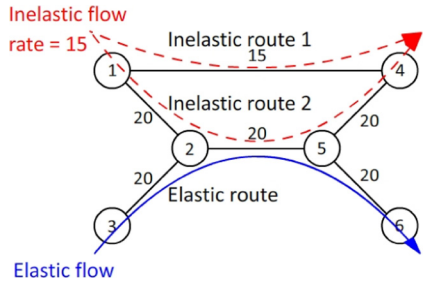

Fig. 2. Topology of the network.

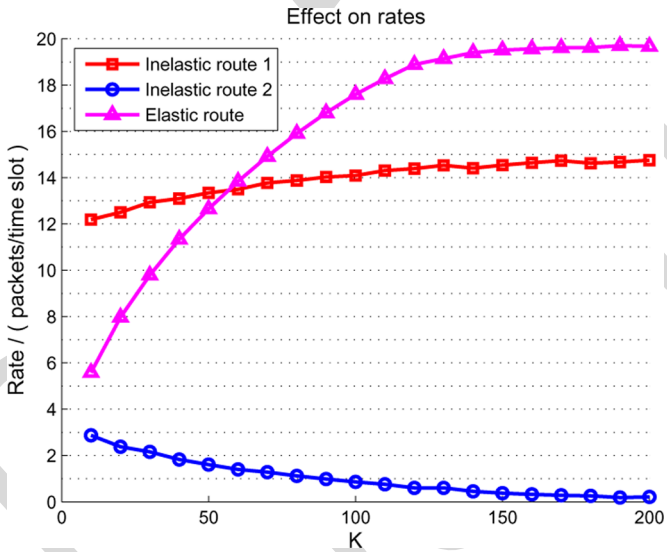

Fig. 3. Effect of K on the average rates on each route of Fig. 2.

V. Simulation Results

In this section, we provide the simulation results for our algorithms under the stochastic model where the arrival process of the inelastic flow f_{i} is such that $A_{\mathrm{i}}[t]$ is Poisson-distributed with mean a_{i} for each t.

A. Effect of the Aggressiveness of the Inelastic Flow

We noted in Section III-B that the factor K represents the "aggressiveness"' of the elastic flows. Also, it is revealed in Proposition 3 that K can be used to control the proximity to the optimal allocation. Here, we test these results for the case of proportionally fair allocation, which corresponds to having the utility function is chosen as [26]: $U_{\mathrm{e}}(x) = \alpha \ln x$, and thus $U_{\mathrm{e}}'^{-1}(\frac{q}{K}) = \frac{\alpha K}{q}$.

In this first set of simulations, we considered the network shown in Fig. 2 with the indicated link capacities and inelastic and elastic flows. Note that the arrival rate of the inelastic flow is $a_{\mathrm{i}} = 15$ to be distributed over the two dashed routes.

The joint algorithm for the SNO-K problem is implemented for this network, and the mean elastic rate allocation is computed for different values of K. Fig. 3 illustrates the effect of K on the rates of the elastic flow and the distribution of the inelastic

IEEE/ACM Transactions on Networking Web Version

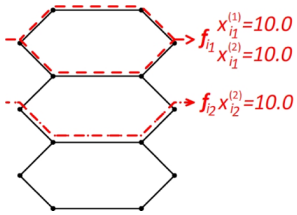

Fig. 4. Phase 1: Two inelastic flows with disjoint routes.

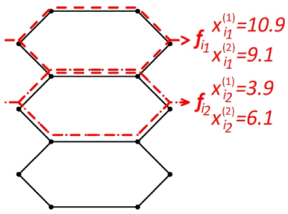

Fig. 5. Phase 2: Two inelastic flows with intersecting routes.

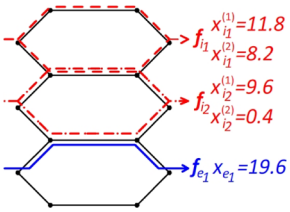

Fig. 6. Phase 3: Two intersecting inelastic flows, and one elastic flow that interacts with them.

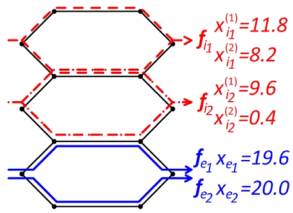

Fig. 7. Phase 4: Two intersecting inelastic flows, and two elastic flows with disjoint routes.

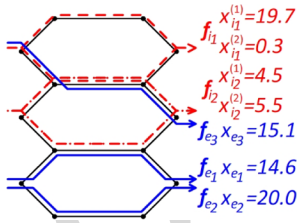

Fig. 8. Phase 5: A third elastic flow enters, which intersects with two inelastic flows.

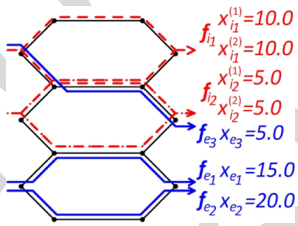

Fig. 9. Performance under static rate distribution for inelastic traffic.

flow's rate over its available routes. We see that as the elastic flow becomes more aggressive, it achieves a higher throughput and thus consumes greater resource on the bottleneck link (2,5). As a reaction to the increased contention from the elastic flow, the load-balancing mechanism of the inelastic flows automatically pushes more and more traffic of the inelastic flow onto route 1.

Note that although increasing the aggressiveness of the elastic flow will increase the utilization of the network, it will result in more delays on the network flows as the queue length over the whole network grows, as shown by Proposition 3. Proposition 3 also suggests that larger K resulting better convergence to the optimal operating point, which is confirmed in the above simulation.

B. More Complex Topology

To illustrate other facets of our algorithm, we conducted our simulation in a more complicated network with different flow assignments. The topology of the network is shown in Fig. 4. The capacity of all the links in the network is 20, and we used elastic flows with identical utility functions and $K = 200$ in our simulation, expecting close-to-optimal utilization (as shown in Fig. 3).

We simulate a sequence of scenarios discussed in five phases. In Phase 1, two disjoint inelastic flows with the routes as shown in Fig. 4 share the network, having rates $a_{\mathrm{i}1} = 20$ and $a_{\mathrm{i}2} = 10$. The average rates provided on each route by our joint algorithm are given in Fig. 4.

When the two inelastic flows share a common bottleneck link in Phase 2, the load-balancing algorithm will shift part of the traffic from the bottleneck link to yield the average rates given in Fig. 5.

In Phase 3, an elastic flow enters the system and shares a link with $f_{\mathrm{i}2}$ as in Fig. 6. We can see from the average rates given in the figure that this elastic flow not only has an effect on $f_{\mathrm{i}2}$, but also shifts the rate of $f_{\mathrm{i}1}$. Here, it can be seen that the interaction between the flows becomes complex even for small networks, and it is not clear what the best allocation is. Yet, through our joint algorithm, $f_{\mathrm{e}1}$ is able to operate dynamically close to the full capacity of all the resources available to it.

After adding another elastic flow $f_{\mathrm{e}2}$ into the network, which is disjoint with all other flows in Phase 4 shown in Fig. 7, we can see that it has no effect on the rates of all other routes, and it fully utilizes that route.

In Phase 5, a third elastic flow $f_{\mathrm{e}3}$ enters and shares common links with both $f_{\mathrm{i}1}$ and $f_{\mathrm{i}2}$, as shown in Fig. 8. We can see that since $f_{\mathrm{e}1}$ also shares links with $f_{\mathrm{i}2}$, $f_{\mathrm{e}3}$ also has effect on it. It can be easily verified that $x_{\mathrm{e}1} = x_{\mathrm{e}3} = 15$ is the optimal operating point, and the average rates achieved by our algorithm are very close to optimal as predicted by Proposition 3.

To study the importance of dynamic load balancing, we also simulated a static rate distribution algorithm as a basis for comparison. This algorithm equally splits the inelastic traffic onto each of its routes (assume it is feasible in the network) and does the congestion control of the elastic flows in the same manner as in our algorithm. This algorithm is implemented for the scenario in Phase 5 with the average rates indicated in Fig. 9. We see that due to the absence of dynamic load balancing, the elastic flows

IEEE Proof Version

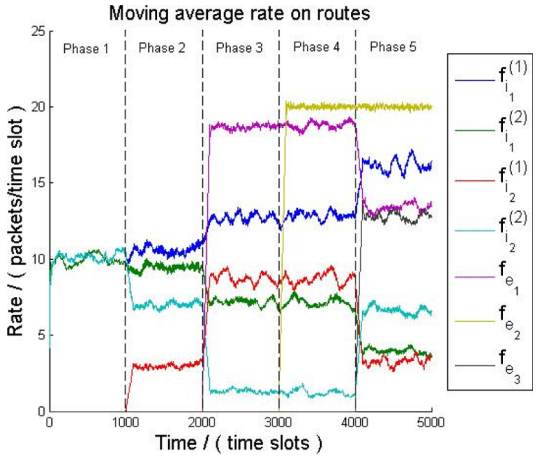

Fig. 10. Injection rate on each route.

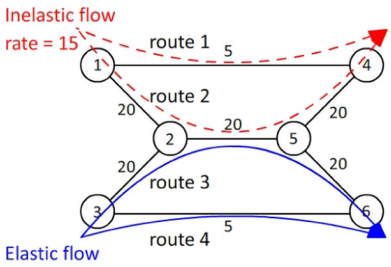

Fig. 11. Network topology for simulating the virtual queue algorithm.

cannot utilize the network fully since the rates assigned to the inelastic flows are fixed. Under the logarithm utility function, this approach achieves a utility of $1.61\alpha K$, while our algorithm achieves $2.71\alpha K$ on the elastic flow f_{e3}.

In this sequence of simulations, we see complex interactions between the elastic and inelastic flows and observed that our algorithm achieves optimal performance distributively. While we have so far focused on the average achieved rates, in Fig. 10, we also show the time evolution of the flow rates on each route as the network goes through the five phases. We see in this figure that the rates converge to their optimal value quickly, which may be important under dynamic conditions.

C. Simulation Using the Virtual Queue Algorithm

In this simulation, we use the joint congestion control and load-balancing algorithm with virtual queue to show the impact of the virtual queue implementation on delay. The simulation is conducted in the network showing in Fig. 11. The parameter ρ_1 was set to 0.95, and ρ_2 was set to 0.9, over all links.

Table I compares the performance with and without virtual queues. First, we note that on link (2,3), though it is critically loaded by two types of flows, the inelastic flow has a much smaller delay compared to the elastic flow due to the strict prioritization. Also, as we can observe, under the original algorithm, route 1 is critically loaded by inelastic flow, resulting in a large delay. With the virtual queue implementation, we manage to decrease the rate on route 1, thus dropping the delay significantly. As one can observe from the table, the delay is greatly

TABLE I
RATE AND DELAY ON EACH ROUTE

	w/o virtual queue		w/ virtual queue	
	rate	delay	rate	delay
route 1	4.9955	40.320	4.4984	0.5405
route 2	9.7414	0.0440	10.502	0.0005
route 3	10.259	15.854	8.5118	1.0137
route 4	4.9950	77.461	4.7817	1.9765

reduced for both elastic and inelastic traffic without a significant degradation in the rate of the elastic traffic. Thus, especially under critical loaded scenarios, virtual queue implementation can achieve significant delay improvements.

Also, for the elastic flows, the delay drops significantly in the tradeoff of a small loss in utilization.

VI. CONCLUSION

In this work, we consider the optimal control of networks that serve heterogeneous traffic types with diverse demands, namely inelastic and elastic traffic. We formulated a new network optimization problem, proposed a novel queueing architecture, and developed a distributed load-balancing and congestion control algorithm with provably optimal performance. We also provided an important improvement to our joint algorithm to achieve better delay performance by introducing new design parameters (ρ_1, ρ_2) together with a set of virtual queues. We have also extended our algorithm to the case of allowing elastic flows to choose their routes dynamically, which will further utilize the resource available in the network.

Future research of this topic includes the following. 1) One future direction is to extend our results to multihop wireless networks with fading channels and interference and develop joint load-balancing/congestion control/routing/scheduling algorithms. 2) Here, we considered a time-slotted system and assumed that the network is perfectly synchronized. The impact of possible asynchronism on the algorithm performance needs to be studied. 3) We adopted a link-centric formulation, which assumes instantaneous arrivals of the packets at all the links on their routes. An alternative is to consider a node-centric formulation, where packets are sequentially transferred, and a source only requires the information of the queues at the source. 4) So far, we have focused on the stability and long-term guarantees for the traffic types. We aim to investigate oscillatory behavior [20] and delay characteristics in our future work. 5) In this work, we assume the routes and the supportability of the inelastic flow are given. Developing corresponding routing and admission control mechanism will make it complete.

APPENDIX A
PROOF OF PROPOSITION 2

Define a Lyapunov function

$$V(\mathbf{p}(t), \mathbf{x}_i(t)) = \frac{1}{2}\sum_{l\in\mathcal{L}} (p_l(t) - \alpha_l^*)^2 + \frac{1}{2}\sum_{f_i\in\mathcal{F}_i}\sum_{r=1}^{|\mathcal{R}_i|}\left(x_i^{(r)}(t) - x_i^{*(r)}\right)^2 \quad (19)$$

IEEE Proof Web Version

where α^* and $\mathbf{x}_{\mathrm{i}}^*$ satisfy conditions (i) and (ii). Note that $\mathbf{x}_{\mathrm{i}}^*$ and α^* may not be unique. Then, we have

$$\begin{aligned}
\frac{d}{dt}V(\mathbf{p}(t),\mathbf{x}_{\mathrm{i}}(t)) &= \sum_{l\in\mathcal{L}}\left(p_l(t)-\alpha_l^*\right)\dot{p}_l(t) \\
&\quad+\sum_{f_i\in\mathcal{F}_{\mathrm{i}}}\sum_{r=1}^{|\mathcal{R}_{\mathrm{i}}|}\left(x_{\mathrm{i}}^{(r)}(t)-x_{\mathrm{i}}^{*(r)}\right)\dot{x}_{\mathrm{i}}^{(r)}(t) \\
&= \sum_{l\in\mathcal{L}}\left(p_l(t)-\alpha_l^*\right)\left(z_l(t)+y_l(t)-c_l\right)_{p_l(t)}^{+} \\
&\quad+\sum_{f_i\in\mathcal{F}_{\mathrm{i}}}\sum_{r=1}^{|\mathcal{R}_{\mathrm{i}}|}\left(x_{\mathrm{i}}^{(r)}(t)-x_{\mathrm{i}}^{*(r)}\right) \\
&\quad\times\left(\bar{q}_{\mathrm{i}}(t)-q_{\mathbf{R}_{\mathrm{i}}^{(r)}}(t)\right)_{x_{\mathrm{i}}^{(r)}(t)}^{+} \\
&\le \sum_{l\in\mathcal{L}}\left(p_l(t)-\alpha_l^*\right)\left(z_l(t)+y_l(t)-c_l\right) \\
&\quad+\sum_{f_i\in\mathcal{F}_{\mathrm{i}}}\sum_{r=1}^{|\mathcal{R}_{\mathrm{i}}|}\left(x_{\mathrm{i}}^{(r)}(t)-x_{\mathrm{i}}^{*(r)}\right) \\
&\quad\times\left(\bar{q}_{\mathrm{i}}(t)-q_{\mathbf{R}_{\mathrm{i}}^{(r)}}(t)\right)_{x_{\mathrm{i}}^{(r)}(t)}^{+} \\
&= \sum_{l\in\mathcal{L}}\left(p_l(t)-\alpha_l^*\right)\left(z_l(t)-z_l^*\right) \\
&\quad+\sum_{l\in\mathcal{L}}\left(p_l(t)-\alpha_l^*\right)\left(y_l(t)+z_l^*-c_l\right) \\
&\quad+\sum_{f_i\in\mathcal{F}_{\mathrm{i}}}\sum_{r=1}^{|\mathcal{R}_{\mathrm{i}}|}\left(x_{\mathrm{i}}^{(r)}(t)-x_{\mathrm{i}}^{*(r)}\right) \\
&\quad\times\left(\bar{q}_{\mathrm{i}}(t)-q_{\mathbf{R}_{\mathrm{i}}^{(r)}}(t)\right)_{x_{\mathrm{i}}^{(r)}(t)}^{+}.
\end{aligned}$$

Next, we show the negativity of the drift term by term. First, we have

$$\begin{aligned}
&\sum_{l\in\mathcal{L}}\left(p_l(t)-\alpha_l^*\right)\left(y_l(t)+z_l^*-c_l\right) \\
&\le \sum_{l\in\mathcal{L}}\left(p_l(t)-\alpha_l^*\right)\left(y_l(t)-y_l^*\right) \\
&= \left(\mathbf{p}^T(t)-\alpha^{*T}\right)\mathbf{R}_{\mathrm{e}}\left(\mathbf{x}_{\mathrm{e}}(t)-\mathbf{x}_{\mathrm{e}}^*\right) \\
&= \left(\mathbf{q}^T(t)-\beta^{*T}\right)\left(\mathbf{x}_{\mathrm{e}}(t)-\mathbf{x}_{\mathrm{e}}^*\right) \\
&= \sum_{f_{\mathrm{e}}\in\mathcal{F}_{\mathrm{e}}}\left(U_{\mathrm{e}}'(x_{\mathrm{e}}(t))-U_{\mathrm{e}}'(x_{\mathrm{e}}^*)\right) \\
&\quad\times\left(x_{\mathrm{e}}(t)-x_{\mathrm{e}}^*\right) \\
&\le 0
\end{aligned} \tag{20}$$

where the first inequality holds because $y_l^*+z_l^*\le c_l$ for any $l\in\mathcal{L}$, and $\alpha_l^*=0$ if $y_l^*+z_l^*<c_l$, $\alpha_l^*>0$ if and only if $y_l^*+z_l^*=c_l$; the second equality holds due to Assumption 1.

Without loss of generality, we assume that $x_{\mathrm{i}}^{*(1)}>0$ for all f_{i}, then we have

$$\begin{aligned}
&\sum_{f_{\mathrm{i}}\in\mathcal{F}_{\mathrm{i}}}\sum_{r=1}^{|\mathcal{R}_{\mathrm{i}}|}\left(x_{\mathrm{i}}^{(r)}(t)-x_{\mathrm{i}}^{*(r)}\right)\left(\bar{q}_{\mathrm{i}}(t)-q_{\mathbf{R}_{\mathrm{i}}^{(r)}}(t)\right)_{x_{\mathrm{i}}^{(r)}(t)}^{+} \\
&\quad+\sum_{l\in\mathcal{L}}\left(p_l(t)-\alpha_l^*\right)\left(z_l(t)-z_l^*\right) \\
&\le \sum_{f_{\mathrm{i}}\in\mathcal{F}_{\mathrm{i}}}\sum_{r=1}^{|\mathcal{R}_{\mathrm{i}}|}\left(x_{\mathrm{i}}^{(r)}(t)-x_{\mathrm{i}}^{*(r)}\right)\left(\bar{q}_{\mathrm{i}}(t)-q_{\mathbf{R}_{\mathrm{i}}^{(r)}}(t)\right) \\
&\quad+\sum_{l\in\mathcal{L}}\left(p_l(t)-\alpha_l^*\right)\left(z_l(t)-z_l^*\right) \\
&= \sum_{f_{\mathrm{i}}\in\mathcal{F}_{\mathrm{i}}}\sum_{r=1}^{|\mathcal{R}_{\mathrm{i}}|}\left(x_{\mathrm{i}}^{(r)}(t)-x_{\mathrm{i}}^{*(r)}\right)\left(\bar{q}_{\mathrm{i}}(t)-q_{\mathbf{R}_{\mathrm{i}}^{(r)}}(t)\right) \\
&\quad+\sum_{l\in\mathcal{L}}\left(p_l(t)-\alpha_l^*\right)\sum_{f_{\mathrm{i}}\in\mathcal{F}_{\mathrm{i}}}\sum_{r=1}^{|\mathcal{R}_{\mathrm{i}}|}\left(x_{\mathrm{i}}^{(r)}(t)-x_{\mathrm{i}}^{*(r)}\right)\mathbf{R}_{\mathrm{i}}^{(r)}[l] \\
&= \sum_{f_{\mathrm{i}}\in\mathcal{F}_{\mathrm{i}}}\sum_{r=1}^{|\mathcal{R}_{\mathrm{i}}|}\left(x_{\mathrm{i}}^{(r)}(t)-x_{\mathrm{i}}^{*(r)}\right)\left(\bar{q}_{\mathrm{i}}(t)-q_{\mathbf{R}_{\mathrm{i}}^{(r)}}(t)\right) \\
&\quad+\sum_{f_{\mathrm{i}}\in\mathcal{F}_{\mathrm{i}}}\sum_{r=1}^{|\mathcal{R}_{\mathrm{i}}|}\sum_{l\in\mathcal{L}}\left(p_l(t)-\alpha_l^*\right)\mathbf{R}_{\mathrm{i}}^{(r)}[l]\left(x_{\mathrm{i}}^{(r)}(t)-x_{\mathrm{i}}^{*(r)}\right) \\
&= \sum_{f_{\mathrm{i}}\in\mathcal{F}_{\mathrm{i}}}\sum_{r=1}^{|\mathcal{R}_{\mathrm{i}}|}\left(x_{\mathrm{i}}^{(r)}(t)-x_{\mathrm{i}}^{*(r)}\right)\left(\bar{q}_{\mathrm{i}}(t)-q_{\mathbf{R}_{\mathrm{i}}^{(r)}}(t)\right) \\
&\quad+\sum_{f_{\mathrm{i}}\in\mathcal{F}_{\mathrm{i}}}\sum_{r=1}^{|\mathcal{R}_{\mathrm{i}}|}\left(x_{\mathrm{i}}^{(r)}(t)-x_{\mathrm{i}}^{*(r)}\right)\left(q_{\mathbf{R}_{\mathrm{i}}^{(r)}}(t)-\beta_{\mathbf{R}_{\mathrm{i}}^{(r)}}^*\right) \\
&= \sum_{f_{\mathrm{i}}\in\mathcal{F}_{\mathrm{i}}}\sum_{r=1}^{|\mathcal{R}_{\mathrm{i}}|}\left(x_{\mathrm{i}}^{(r)}(t)-x_{\mathrm{i}}^{*(r)}\right)\left(\bar{q}_{\mathrm{i}}(t)-\beta_{\mathbf{R}_{\mathrm{i}}^{(r)}}^*\right) \\
&\le_{(a)} \sum_{f_{\mathrm{i}}\in\mathcal{F}_{\mathrm{i}}}\left(\left(\bar{q}_{\mathrm{i}}(t)-\beta_{\mathbf{R}_{\mathrm{i}}^{(1)}}^*\right)\sum_{r=1}^{|\mathcal{R}_{\mathrm{i}}|}\left(x_{\mathrm{i}}^{(r)}(t)-x_{\mathrm{i}}^{*(r)}\right)\right) \\
&=_{(b)} 0
\end{aligned} \tag{21}$$

where inequality (a) holds due to Lemma 1, and equality (b) holds due to the equality (10).

Thus, from inequalities (20) and (21), we can conclude that

$$\frac{d}{dt}V(\mathbf{p}(t),\mathbf{x}_{\mathrm{i}}(t))\le 0$$

for all t. Further more, from inequality (20), we also know that $\frac{d}{dt}V(\mathbf{p}(t),\mathbf{x}_{\mathrm{i}}(t))=0$ if and only if $\mathbf{x}_{\mathrm{e}}(t)=\mathbf{x}_{\mathrm{e}}^*$.

Appendix B
Proof of Proposition 5

We construct a partial Lagrangian to solve the FNO-DR problem. Let λ_l and μ_i^d be the Lagrange multipliers associated with the constraints (15) and (17), respectively. Furthermore, let $\boldsymbol{\lambda}=\{\lambda_l\}_l$ and $\boldsymbol{\mu}=\{\mu_i^d\}_{id}$ be the respective vectors; the partial Lagrangian can be written as

$$\begin{aligned}
L(\mathbf{x},\mathbf{r},\boldsymbol{\lambda},\boldsymbol{\mu}) &= \sum_{s,d\in\mathcal{N}}U_s^d\left(x_s^d\right)-\sum_{l\in\mathcal{L}}\lambda_l(y_l+z_l-c_l) \\
&\quad-\sum_{i,d\in\mathcal{N}}\mu_i^d\left(x_i^d+\sum_{m\in\mathcal{N}}r_{mi}^d-\sum_{j\in\mathcal{N}}r_{ij}^d\right)
\end{aligned}$$

IEEE Proof Web Version

$$= \sum_{s,d} \left(U_s^d(x_s^d) - \mu_s^d x_s^d\right) + \sum_d \left(\sum_{(i,j)\in\mathcal{L}} r_{ij}^d \left(\mu_i^d - \mu_j^d - \lambda_{ij}\right)\right) - \sum_l \lambda_l z_l + \sum_l \lambda_l c_l.$$

This problem satisfies Slater's condition, thus *strong duality* holds. From the optimality conditions, we know that the optimal solution $(\mathbf{x}^*, \mathbf{r}^*, \boldsymbol{\lambda}^*, \boldsymbol{\mu}^*)$ must satisfy the following conditions:

$$y_l^* + z_l^* \le c_l \qquad \forall\, l \in \mathcal{L} \tag{22}$$

$$x_i^{*d} + \sum_m r_{mi}^{*d} - \sum_j r_{ij}^{*d} \le 0 \qquad \forall\, i,d \in \mathcal{L} \tag{23}$$

$$x_s^{*d} = (U_s^d)'^{-1}\left(\mu_s^{*d}\right) \qquad \forall\, s,d \in \mathcal{N} \tag{24}$$

$$r_{ij}^{*d} \in, \arg\max_{0\le r_{ij}^d \le P} \sum_d \left(\sum_{(i,j)\in\mathcal{L}} r_{ij}^d \left(\mu_i^{*d} - \mu_j^{*d} - \lambda_{ij}^*\right)\right) \tag{25}$$

$$\lambda_l^* \left(y_l^* + z_l^* - c_l^*\right) = 0 \qquad \forall\, l \in \mathcal{L} \tag{26}$$

$$\mu_i^{*d}\left(x_i^{*d} + \sum_{m\in\mathcal{N}} r_{mi}^{*d} - \sum_{j\in\mathcal{N}} r_{ij}^{*d}\right) = 0 \qquad \forall\, i,d \in \mathcal{N} \tag{27}$$

where (22) and (23) are the primal feasibility, (24) and (25) are the primal optimality condition, and (25)–(27)***[(25) is mentioned twice. Is this correct?]*** are the complementary slackness condition.

Define a Lyapunov function

$$V(\mathbf{p}(t),\mathbf{s}(t),\mathbf{x}_i(t),\mathbf{r}(t)) = \frac{1}{2}\sum_{l\in\mathcal{L}} \left(p_l(t) - \lambda_l^*\right)^2 + \frac{1}{2}\sum_{f_i\in\mathcal{F}_i}\sum_{r=1}^{|\mathcal{R}_i|}\left(x_i^{(r)}(t) - x_i^{*(r)}\right)^2 + \frac{1}{2}\sum_{i,d\in\mathcal{N}}\left(s_i^d(t) - \mu_i^{*d}\right)^2 + \frac{1}{2}\sum_{(i,j)\in\mathcal{L},d\in\mathcal{N}}\left(r_{ij}^d(t) - r_{ij}^{*d}\right)^2.$$

Then, its drift is given by the following (from here, we omit the time index (t) for brevity):

$$\frac{d}{dt}V(\mathbf{p},\mathbf{s},\mathbf{x}_\mathrm{i},\mathbf{r}) = \sum_l \left(p_l - \lambda_l^*\right)\left(z_l + y_l - c_l\right)_{p_l}^+ + \sum_{f_\mathrm{i}\in\mathcal{F}_\mathrm{i}}\sum_{r=1}^{|\mathcal{R}_\mathrm{i}|}\left(x_\mathrm{i}^{(r)} - x_\mathrm{i}^{*(r)}\right) \times \left(\bar{q}_\mathrm{i} - q_{\mathbf{R}_\mathrm{i}^{(r)}}\right)_{x_\mathrm{i}^{(r)}}^+ + \sum_{i,d}\left(s_i^d - \mu_i^{*d}\right) \times \left(x_i^d + \sum_m r_{mi}^d - \sum_j r_{ij}^d\right)_{s_i^d}^+ + \sum_{(i,j),d}\left(r_{ij}^d - r_{ij}^{*d}\right)\dot{r}_{ij}^d$$

$$\le \sum_{l\in\mathcal{L}}\left(p_l - \lambda_l^*\right)\left(z_l - z_l^*\right) \tag{28}$$

$$+ \sum_{l\in\mathcal{L}}\left(p_l - \lambda_l^*\right)\left(y_l + z_l^* - c_l\right) \tag{29}$$

$$+ \sum_{f_\mathrm{i}\in\mathcal{F}_\mathrm{i}}\sum_{r=1}^{|\mathcal{R}_\mathrm{i}|}\left(x_\mathrm{i}^{(r)} - x_\mathrm{i}^{*(r)}\right) \times \left(\bar{q}_\mathrm{i} - q_{\mathbf{R}_\mathrm{i}^{(r)}}\right) \tag{30}$$

$$+ \sum_{i,d}\left(s_i^d - \mu_i^{*d}\right) \times \left(x_i^d + \sum_m r_{mi}^d - \sum_j r_{ij}^d\right) \tag{31}$$

$$+ \sum_{(i,j),d}\left(r_{ij}^d - r_{ij}^{*d}\right)\left(s_i^d - s_j^d - p_{ij}\right). \tag{32}$$

Next, we show the negativity of the drift. First, from the proof of the fixed route scenario, we know that $(28)+(30) \le 0$ follows the same reasoning there

$$(29) + (30) \le \sum_{(i,j)\in\mathcal{L}}\left(p_{ij} - \lambda_{ij}^*\right)\left(\sum_d r_{ij}^d - \sum_d r_{ij}^{*d}\right) + \sum_{i,d}\left(s_i^d - \mu_i^{*d}\right)\left(x_i^d + \sum_m r_{mi}^d - \sum_j r_{ij}^d\right)$$

$$= \sum_{(i,j)\in\mathcal{L}}\left(p_{ij} - \lambda_{ij}^*\right)\left(\sum_d r_{ij}^d - \sum_d r_{ij}^{*d}\right) \tag{33}$$

$$+ \sum_{i,d}\left(s_i^d - \mu_i^{*d}\right)\left(x_i^d - x_i^{*d}\right) \tag{34}$$

$$+ \sum_{i,d}\left(s_i^d - \mu_i^{*d}\right)\left(x_i^{*d} + \sum_m r_{mi}^d - \sum_j r_{ij}^d\right). \tag{35}$$

Notice that

$$(34) = \sum_{i,d}\left(\left(U_s^d\right)'\left(x_i^d\right) - \left(U_s^d\right)'\left(x_i^{*d}\right)\right)\left(x_i^d - x_i^{*d}\right)$$

and the assumption that the utility function U_s^d is a concave function, we have $(37) \le 0$. By adding and subtracting the same term $\sum_{i,d}\left(\mu_i^{*d}\left(\sum_m r_{mi}^{*d} - \sum_j r_{ij}^{*d}\right)\right)$ to the rest of the terms, we get

$$(33) + (35) = \sum_{(i,j),d} p_{ij} r_{ij}^d - \sum_{(i,j),d} p_{ij} r_{ij}^{*d} - \sum_{(i,j),d}\lambda_{ij}^* r_{ij}^d \tag{36}$$

$$+ \sum_{(i,j),d}\lambda_{ij}^* r_{ij}^{*d} \tag{37}$$

$$+ \sum_{i,d}\left(x_i^{*d} s_i^d + s_i^d\left(\sum_m r_{mi}^d - \sum_j r_{ij}^d\right)\right) \tag{38}$$

IEEE Proof Web version

$$-\sum_{i,d}\left(x_i^{*d}\mu_i^{*d}+\mu_i^{*d}\left(\sum_m r_{mi}^{*d}-\sum_j r_{ij}^{*d}\right)\right) \quad (39)$$

$$+\sum_{i,d}\left(\mu_i^{*d}\left(\sum_m r_{mi}^{*d}-\sum_j r_{ij}^{*d}\right)\right) \quad (40)$$

$$-\sum_{i,d}\left(\mu_i^{*d}\left(\sum_m r_{mi}^{d}-\sum_j r_{ij}^{d}\right)\right). \quad (41)$$

Note that $(39)=0$ by (27). Combine the first term in (36) with (38), the third term with (41) and (37) with (40), and we get

$$\begin{aligned}
(33)+(35)=&-\sum_{(i,j),d} p_{ij}r_{ij}^{*d}\\
&+\left(\sum_{i,d}x_i^{*d}s_i^d-\sum_{(i,j),d}r_{ij}^d\left(s_i^d-s_j^d-p_{ij}\right)\right)\\
&-\left(\sum_{(i,j),d}r_{ij}^{*d}\left(\mu_i^{*d}-\mu_j^{*d}-\lambda_{ij}^*\right)\right)\\
&+\left(\sum_{(i,j),d}r_{ij}^{d}\left(\mu_i^{*d}-\mu_j^{*d}-\lambda_{ij}^*\right)\right)\\
\le_{(a)}&-\sum_{(i,j),d}p_{ij}r_{ij}^{*d}\\
&+\left(\sum_{i,d}x_i^{*d}s_i^d-\sum_{(i,j),d}r_{ij}^d\right.\\
&\left.\times\left(s_i^d-s_j^d-p_{ij}\right)\right)\\
\le_{(b)}&\sum_{i,d}\left(\sum_j r_{ij}^{*d}-\sum_m r_{mi}^{*d}\right)s_i^d\\
&-\sum_{(i,j),d}p_{ij}r_{ij}^{*d}-\sum_{(i,j),d}r_{ij}^d\\
&\times\left(s_i^d-s_j^d-p_{ij}\right)\\
=&\sum_{(i,j),d}r_{ij}^{*d}\left(s_i^d-s_j^d-p_{ij}\right)\\
&-\sum_{(i,j),d}r_{ij}^d\left(s_i^d-s_j^d-p_{ij}\right)\\
=&-(32)
\end{aligned}$$

where (a) holds since r_{ij}^{*d} maximizes $\sum_{(i,j),d}r_{ij}^d\left(\mu_i^{*d}-\mu_j^{*d}-\lambda_{ij}^*\right)$ over all r_{ij}^d, thus $\sum_{(i,j),d}r_{ij}^{*d}\left(\mu_i^{*d}-\mu_j^{*d}-\lambda_{ij}^*\right)\ge\sum_{(i,j),d}r_{ij}^{d}\left(\mu_i^{*d}-\mu_j^{*d}-\lambda_{ij}^*\right)$ and (b) holds follow from (23).

Thus, we conclude that

$$\frac{d}{dt}V(\mathbf{p}(t),\mathbf{s}(t),\mathbf{x_i}(t),\mathbf{r}(t))\le 0$$

for all t, and the equality holds if and only if $\mathbf{x}_e(t)=\mathbf{x}_e^*$.

REFERENCES

[1] E. Altman, T. Başar, and R. Srikant, "Congestion control as a stochastic control problem with action delays," *Automatica*, vol. 35, pp. 1937–1950, 1999.

[2] J. Bolot and A. Shankar, "Dynamic behavior of rate-based flow cntrol mechanisms," *ACM Comput. Commun. Rev.*, vol. 20, no. 2, 1992***[Pages?]***.

[3] S. Borst and N. Hegde, "Integration of streaming and elastic traffic in wireless networks," in *Proc. IEEE INFOCOM*, May 2007, pp. 1884–1892.

[4] S. Boyd and L. Vandenberghe, *Convex Optimization*. Cambridge, U.K.: Cambridge Univ. Press, 2004.

[5] L. Bui, A. Eryilmaz, R. Srikant, and X. Wu, "Joint asynchronous congestion control and distributed scheduling for wireless networks," in *Proc. IEEE INFOCOM*, 2006.

[6] A. Eryilmaz and R. Srikant, "Fair resource allocation in wireless networks using queue-length based scheduling and congestion control," in *Proc. IEEE INFOCOM*, Miami, FL, Mar. 2005, vol. 3, pp. 1794–1803.

[7] A. Eryilmaz and R. Srikant, "Resource allocation of multi-hop wireless networks," in *Proc. Int. Zurich Seminar Commun.*, Feb. 2006***[Pages?]***.

[8] A. Eryilmaz, R. Srikant, and J. R. Perkins, "Stable scheduling policies for fading wireless channels," *IEEE/ACM Trans. Networking*, vol. 13, no. 2, pp. 411–425, Apr. 2005.

[9] L. Georgiadis, M. J. Neely, and L. Tassiulas, *Resource Allocation and Cross-Layer Control in Wireless Networks*, ser. Foundations and Trends in Networking. Hanover, MA: now, 2006.

[10] P. Hande, S. Zhang, and M. Chiang, "Distributed rate allocation for inelastic flows," *IEEE/ACM Trans. Netw.*, vol. 15, no. 6, pp. 1240–1253, Dec. 2007.

[11] K. Kar, S. Sarkar, and L. Tassiulas, "A simple rate control algorithm for maximizing total user utillity," in *Proc. IEEE INFOCOM*, Anchorage, AK, 2001, vol. 1, pp. 133–141.

[12] F. P. Kelly, A. Maulloo, and D. Tan, "Rate control in communication networks: Shadow prices, proportional fairness and stability," *J. Oper. Res. Soc.*, vol. 49, pp. 237–252, 1998.

[13] S. Kunniyur and R. Srikant, "An adaptive virtual queue (AVQ) algorithm for active queue management," *IEEE/ACM Trans. Netw.*, vol. 12, no. 2, pp. 286–299, Apr. 2004.

[14] J. Lee, R. R. Mazumdar, and N. Shroff, "Non-convex optimization and rate control for multi-class services in the internet," *IEEE/ACM Trans. Netw.*, vol. 13, no. 4, pp. 827–840, Aug. 2005.

[15] R. Li, A. Eryilmaz, L. Ying, and N. B. Shroff, "A unified approach to optimizing performance in networks serving heterogeneous flows," in *Proc. IEEE INFOCOM*, 2009, pp. 253–261.

[16] X. Lin and N. Shroff, "Joint rate control and scheduling in multihop wireless networks," in *Proc. IEEE CDC*, Paradise Island, Bahamas, Dec. 2004, vol. 2, pp. 1484–1489.

[17] X. Lin and N. Shroff, "The impact of imperfect scheduling on cross-layer rate control in multihop wireless networks," in *Proc. IEEE INFOCOM*, Miami, FL, Mar. 2005, vol. 3, pp. 1804–1814.

[18] X. Lin, N. B. Shroff, and R. Srikant, "A tutorial on cross-layer optimization in wireless networks," *IEEE J. Sel. Areas Commun.*, vol. 24, no. 8, pp. 1452–1463, Aug. 2006.

[19] S. H. Low and D. E. Lapsley, "Optimization flow control, I: Basic algorithm and convergence," *IEEE/ACM Trans. Netw.*, vol. 7, no. 6, pp. 861–875, Dec. 1999.

[20] E. Mallada and F. Paganini, "Stability of node-based multipath routing and dual congestion control," in *Proc. 47th IEEE CDC*, Dec. 2008, pp. 1398–1403.

[21] M. Neely, E. Modiano, and C. Li, "Fairness and optimal stochastic control for heterogeneous networks," in *Proc. IEEE INFOCOM*, Miami, FL, Mar. 2005, pp. 1723–1734.

[22] M. Neely, E. Modiano, and C. Rohrs, "Dynamic power allocation and routing for time varying wireless networks," in *Proc. IEEE INFOCOM*, Apr. 2003, pp. 745–755.

[23] S. Patil and G. Veciana, "Managing resources and quality of service in heterogeneous wireless systems exploiting opportunism," *IEEE/ACM Trans. Netw.*, vol. 15, no. 5, pp. 1046–1058, Oct. 2007.

[24] D. Qiu and N. B. Shroff, "A predictive flow control scheme for efficient network utilization and QoS," *IEEE/ACM Trans. Netw.*, vol. 12, no. 1, pp. 161–172, Feb. 2004.

[25] S. Shakkottai and A. Stolyar, "Scheduling algorithms for a mixture of real-time and non-real-time data in hdr," in *Proc. 17th ITC*, 2001, pp. 793–804.

IEEE Proof Web Version

[26] R. Srikant, *The Mathematics of Internet Congestion Control*. Boston, MA: Birkhäuser, 2004.
[27] A. Stolyar, "Maximizing queueing network utility subject to stability: Greedy primal-dual algorithm," *Queue. Syst.*, vol. 50, no. 4, pp. 401–457, 2005.
[28] L. Tassiulas and A. Ephremides, "Stability properties of constrained queueing systems and scheduling policies for maximum throughput in multihop radio networks," *IEEE Trans. Autom. Control*, vol. 36, no. 12, pp. 1936–1948, Dec. 1992.
[29] X. Wu and R. Srikant, "Regulated maximal matching: A distributed scheduling algorithm for multi-hop wireless networks with node-exclusive spectrum sharing," in *Proc. IEEE CDC*, 2005, pp. 5342–5347.
[30] L. Ying, R. Srikant, A. Eryilmaz, and G. E. Dullerud, "Distributed fair resource allocation in cellular networks in the presence of heterogeneous delays," in *Proc. WiOPT*, 2005, pp. 96–105.

Ruogu Li (S'10) received the B.S. degree in electronic engineering from Tsinghua University, Beijing, China, in 2007, and is currently pursuing the Ph.D. degree in electrical and computer engineering at the Ohio State University, Columbus.

His research interests include optimal network control, wireless communication networks, low-delay scheduling scheme design, and cross-layer algorithm design.

Atilla Eryilmaz (S'00–M'06) received the M.S. and Ph.D. degrees in electrical and computer engineering from the University of Illinois at Urbana-Champaign in 2001 and 2005, respectively.

Between 2005 and 2007, he worked as a Post-Doctoral Associate with the Laboratory for Information and Decision Systems, Massachusetts Institute of Technology, Cambridge. He is currently an Assistant Professor of electrical and computer engineering with the Ohio State University, Columbus. His research interests include communication networks, optimal control of stochastic networks, optimization theory, distributed algorithms, stochastic processes, and network coding.

Dr. Eryilmaz received the National Science Foundation CAREER Award in 2010.

Lei Ying (M'07) received the B.E. degree from Tsinghua University, Beijing, China, in 2001, and the M.S. and Ph.D. degrees in electrical engineering from the University of Illinois at Urbana-Champaign in 2003 and 2007, respectively.

During Fall 2007, he worked as a Post-Doctoral Fellow with the University of Texas at Austin. He is currently an Assistant Professor with the Department of Electrical and Computer Engineering, Iowa State University, Ames, where he is named the Litton Assistant Professor for 2010–2011. His research interest is broadly in the area of information networks, including wireless networks, mobile ad hoc networks, P2P networks, and social networks.

Dr. Ying received a Young Investigator Award from the Defense Thread Reduction Agency (DTRA) in 2009, and a National Science Foundation CAREER Award in 2010.

Ness B. Shroff (S'91–M'93–SM'01–F'07) received the Ph.D. degree from Columbia University, New York, NY, in 1994.

He is currently the Ohio Eminent Scholar of Networking and Communications and a Professor of electrical and computer engineering (ECE) and computer science and engineering with the Ohio State University, Columbus. He also currently serves as a Guest Chaired Professor of wireless communications with the Department of Electronic Engineering, Tsighnua University, Beijing, China. Previously, he was a Professor of ECE with Purdue University, West Lafayette, IN, and the Director of the Center for Wireless Systems and Applications (CWSA), a university-wide center on wireless systems and applications. His research interests span the areas of wireless and wireline communication networks, where he investigates fundamental problems in the design, performance, pricing, and security of these networks.

Dr. Shroff has received numerous awards for his networking research, including the National Science Foundation CAREER award, the Best Paper awards for IEEE INFOCOM 2006 and 2008, the Best Paper Award for IEEE IWQoS 2006, the Best Paper of the Year Award for *Computer Networks*, and the Best Paper of the Year Award for the *Journal of Communications and Networks* (his IEEE INFOCOM 2005 paper was one of two runner-up papers).

IEEE Proof
Web Version

A Unified Approach to Optimizing Performance in Networks Serving Heterogeneous Flows

Ruogu Li, *Student Member, IEEE*, Atilla Eryilmaz, *Member, IEEE*, Lei Ying, *Member, IEEE*, and Ness B. Shroff, *Fellow, IEEE*

***Abstract*—We study the optimal control of communication networks in the presence of heterogeneous traffic requirements. Specifically, we distinguish the flows into two crucial classes: *inelastic* for modeling high-priority, delay-sensitive, and fixed-throughput applications; and *elastic* for modeling low-priority, delay-tolerant, and throughput-greedy applications. We note that the coexistence of such diverse flows creates complex interactions at multiple levels (e.g., flow and packet levels), which prevent the use of earlier design approaches that dominantly assume homogeneous traffic. In this work, we develop the mathematical framework and novel design methodologies needed to support such heterogeneous requirements and propose provably optimal network algorithms that account for the multilevel interactions between the flows. To that end, we first formulate a network optimization problem that incorporates the above throughput and service prioritization requirements of the two traffic types. We, then develop a distributed joint load-balancing and congestion control algorithm that achieves the dual goal of maximizing the aggregate utility gained by the elastic flows while satisfying the fixed throughput and prioritization requirements of the inelastic flows. Next, we extend our joint algorithm in two ways to further improve its performance: in delay through a virtual queue implementation with minimal throughput degradation and in utilization by allowing for dynamic multipath routing for elastic flows. A unique characteristic of our proposed dynamic routing solution is the novel two-stage queueing architecture it introduces to satisfy the service prioritization requirement.**

***Index Terms*—*[Author, please supply index terms/keywords for your paper. To download the IEEE Taxonomy go to http://www.ieee.org/documents/2009Taxonomy_v101.pdf]*.

I. Introduction

OVER the last several years, we have witnessed the development of increasingly sophisticated optimization and control techniques to address a variety of resource allocation problems for communication networks (e.g., [1], [2], [6], [7], [11], [12], [14], [16], [19], [21], [24], and [27]; see [9] and [18] for an overview). Much of this investigation has focused primarily on optimizing functions of long-term performance metrics such as throughput subject to network stability. Two types of traffic can be distinguished: elastic traffic with controllable packet injection rates generated by file transfer or other delay-tolerant applications, and inelastic traffic with fixed packet injection rates generated by delay-sensitive applications. Much of the existing work focuses on the existence of either the inelastic (e.g., [8], [22], and [28]) or the elastic (e.g., [6], [7], [12], [17], and [21]) traffic alone. The integration of elastic and inelastic flows in single-hop wireless systems has been studied in [3], [23], and [25] and has been extended to a multiple-hop network in [10], [14], and [27], however with the restriction of every flow having a single route. In [27], the coexistence of inelastic and elastic flows has also been considered in a more general setup.

However, previous utility maximization-based solutions do not distinguish inelastic packets and elastic packets at the packet level. Thus, the inelastic packets need to compete with elastic packets for link bandwidths, so these two types of flows have comparable delay performance. Yet, inelastic flows model delay-sensitive traffic and must be served with higher priority as they traverse the network. Our framework differs from earlier utility maximization-based approaches in that we give strictly higher service priority to inelastic packets, i.e., at every link, elastic packets can be transmitted only when there are no inelastic packets waiting for service. This prioritization decouples the inelastic packets and elastic packets at the *link (or, equivalently, packet) level* and will result in small delays for inelastic flows. Note that even though two types of flows are decoupled at the link level, to provide high utilization for elastic traffic, the inelastic flows must smartly distribute their load among their available routes. To that end, we developed our algorithm to maximize the network utility defined by elastic flows under the prioritization, which provides new coupling methods at the *flow level* that are different from previous utility maximization-based solutions.

We believe the main contributions of this work to be the following.

- The mathematical formulation of the utility maximization problem for elastic rate control subject to inelastic traffic requirements of fixed rate and service prioritization.
- The development of a distributed joint load-balancing and rate-control algorithm that gives strict service priority to inelastic packets while guaranteeing optimal resource utilization for elastic traffic. The description and the opti-

Manuscript received September 07, 2009; revised March 22, 2010 and June 11, 2010; accepted June 24, 2010; approved by IEEE/ACM TRANSACTIONS ON NETWORKING Editor E. Modiano. This work was supported in part by DTRA Grants HDTRA1-08-1-0016 and HDTRA1-09-1-0055, ARO MURI Award W911NF-08-1-0238, and NSF Awards 0626703-CNS, 0635202-CCF, 0721236-CNS, 08-31756, 09-53165, 953515-CNS, and 0916664-CCF. An earlier version of this work appeared in the *Proceedings of IEEE INFOCOM*, April 2009.

R. Li, A. Eryilmaz, and N. B. Shroff are with the Department of Electrical and Computer Engineering, The Ohio State University, Columbus, OH 43210 USA (e-mail: lir@ece.osu.edu; eryilmaz@ece.osu.edu; shroff@ece.osu.edu).

L. Ying is with the Department of Electrical and Computer Engineering, Iowa State University, Ames, IA 50010 USA (e-mail: leiying@engineering.iastate.edu).

Color versions of one or more of the figures in this paper are available online at http://ieeexplore.ieee.org.

Digital Object Identifier 10.1109/TNET.2010.2059038

1063-6692/$26.00 © 2010 IEEE

IEEE Proof Print Version

mality of this algorithm are provided for both the fluid model and the actual stochastic network.
- The extension of the base algorithm to a virtual queue-based operation that enables further delay reduction for both traffic types with a nominal and controllable sacrifice in the network utilization.
- The relaxation of the static route assumption for the elastic flows to achieve higher utilization of the network resources through dynamic, multipath routing while maintaining the prioritization requirements. This leads to a novel two-stage queueing architecture that complies with the prioritization requirements of the design.

The rest of the paper is organized as follows. We introduce our system model and formulate the main stochastic network optimization problem in Section II. In Section III, we first analyze a simple fluid version of the problem, and then using the insights gained to extend the solution to the stochastic scenario. In Section IV, we extend the algorithm in two practically important directions that improve delay performance and allow for dynamic multipath routing for elastic traffic. The simulation results and our concluding remarks are provided in Sections V and VI, respectively.

II. System Model and Objectives

We consider a fixed network represented by a graph $\mathcal{G} = (\mathcal{N}, \mathcal{L})$, where $\mathcal{N}$ is the set of nodes and $\mathcal{L}$ is the set of directed links. We assume that the capacity of link $l \in \mathcal{L}$ is c_l, and define the vector of link capacities as $\mathbf{c} := (c_l)_{l\in\mathcal{L}}$. Time is slotted in our system, and the external packets arrive at the beginning of each time slot.

We consider the scenario where the network resources are shared by a set of *inelastic* and *elastic flows*, where a flow is defined by its source node and destination node. While the inelastic flow represents traffic with fixed rates and stringent delay constraints such as voice and video streaming, the elastic flow represents delay-tolerant traffic with adaptive rates such as non-real-time file sharing and e-mail applications. The set of all flows in the network is denoted by $\mathcal{F}$, which is partitioned into two subsets, $\mathcal{F}_e$ and $\mathcal{F}_i$, where $\mathcal{F}_\mathrm{e}$ is the set of elastic flows and $\mathcal{F}_\mathrm{i}$ is the set of inelastic flows. Next, we describe the characteristics of inelastic and elastic flows in more detail.

Inelastic Flow: We let f_i denote an inelastic flow in the network with source s_i and destination d_i. Each inelastic flow f_i is associated with a fixed set of routes $\mathcal{R}_\mathrm{i}$. The rth route of this set is described by a vector $\mathbf{R}_\mathrm{i}^{(r)}$ such that $\mathbf{R}_\mathrm{i}^{(r)}[l] = 1$ if link $l \in \mathcal{L}$ is on that route, and zero otherwise. Let $x_\mathrm{i}^{(r)}[t]$ be the number of injected packets on the rth route of flow f_i at time slot t, and let $\mathbf{x}_\mathrm{i}[t] := \left(x_\mathrm{i}^{(r)}[t]\right)_{f_\mathrm{i}\in\mathcal{F}_\mathrm{i}}^{\mathbf{R}^{(r)}\in\mathcal{R}_\mathrm{i}}$ be the vector of inelastic flow packets injected on each route in slot t. Note that we slightly abuse our notation by using $\mathbf{x}_\mathrm{i}$ to denote rate vector of all inelastic flows, while $x_\mathrm{i}^{(r)}$ stands for the rate of flow $f_\mathrm{i} \in \mathcal{F}_\mathrm{i}$ over route $r \in \mathcal{R}_\mathrm{i}$. We assume that the packet arrivals of the inelastic flow f_i follow a stochastic process $A_\mathrm{i}[t]$ that is identically and independently distributed (*i.i.d.*) over time with a fixed mean rate, denoted by $a_\mathrm{i} := \mathbb{E}(A_\mathrm{i}[t])$, and a finite second moment, i.e., $\mathbb{E}\left(A_\mathrm{i}^2[t]\right) < \infty$.

To clarify the difference between $A_\mathrm{i}[t]$ and $\left(x_\mathrm{i}^{(r)}[t]\right)_{r\in\mathcal{R}_\mathrm{i}}$, we note that $A_\mathrm{i}[t]$ denotes the number of packets *generated* by flow f_i while $\left(x_\mathrm{i}^{(r)}[t]\right)_{r\in\mathcal{R}_\mathrm{i}}$ describes the number of packets *injected* into the network to traverse each of the available routes of flow f_i. Thus, $A_\mathrm{i}[t]$ is an uncontrollable stochastic process describing exogenous arrivals, whereas $\left(x_\mathrm{i}^{(r)}[t]\right)_{r\in\mathcal{R}_\mathrm{i}}$ is controllable by the network algorithm.

For notational convenience, we define

$$z_l(\mathbf{x}_\mathrm{i}[t]) := \sum_{f_\mathrm{i}\in\mathcal{F}_\mathrm{i}} \sum_{r=1}^{|\mathcal{R}_\mathrm{i}|} x_\mathrm{i}^{(r)}[t]\mathbf{R}_\mathrm{i}^{(r)}[l]$$

to denote the total number of inelastic packets on link l for a given $\mathbf{x}_\mathrm{i}[t]$.

Elastic Flow: We let f_e denote an elastic flow in the network with source s_e and destination d_e. In Section IV-B, we will consider dynamic routing for the elastic flow, but for now we will concentrate on the fix route case to get some insight about the load balancing. Here, we assume that each elastic flow f_e is associated with a single route $\mathbf{R}_\mathrm{e}$, and we let $x_\mathrm{e}[t]$ be the number of injected packets of flow f_e in slot t. Similar to the inelastic case, we also define $\mathbf{x}_\mathrm{e}[t] := (x_\mathrm{e}[t])_{f_\mathrm{e}\in\mathcal{F}_\mathrm{e}}$ to be the vector of elastic flow rates in slot t, and

$$y_l(\mathbf{x}_\mathrm{e}[t]) := \sum_{f_\mathrm{e}\in\mathcal{F}_\mathrm{e}} x_\mathrm{e}[t]\mathbf{R}_\mathrm{e}[l]$$

to denote the total number of elastic packets on link l. Associated with each elastic flow f_e, there exists a utility function $U_\mathrm{e}(\cdot)$ that measures the "satisfaction" of that flow as a function of its mean injection rate $\bar{x}_\mathrm{e} := \lim_{T\to\infty} \frac{1}{T}\sum_{t=0}^{T-1} x_\mathrm{e}[t]$. We also assume that the sources of the elastic flows are always infinitely backlogged.[1]

In the text, we use $\mathbf{x}[t] := (\mathbf{x}_\mathrm{i}[t], \mathbf{x}_\mathrm{e}[t])$ to denote the vector of inelastic and elastic packets injected into the network in slot t. Next, we provide a set of assumptions to be used later in the analysis.

Assumption 1: The elastic routing matrix $[\mathbf{R}_\mathrm{e}]_{f_\mathrm{e}\in\mathcal{F}_\mathrm{e}}$ has full row rank, which guarantees that given $\mathbf{q}$, there exists a unique $\mathbf{p}$ such that $\mathbf{q} = ([\mathbf{R}_\mathrm{e}]_{f_\mathrm{e}\in\mathcal{F}_\mathrm{e}})^T\mathbf{p}$.

Assumption 2: The inelastic arrival process $\{A_\mathrm{i}[t]\}_{f_\mathrm{i}\in\mathcal{F}_\mathrm{i}}$ is such that there exists a vector $\mathbf{x}_\mathrm{i}$ satisfying

$$\sum_{r=1}^{|\mathcal{R}_\mathrm{i}|} x_\mathrm{i}^{(r)} = a_\mathrm{i} \forall\ f_\mathrm{i} \in \mathcal{F}_\mathrm{i} \quad \text{and} \quad z_l(\mathbf{x}_\mathrm{i}) < c_l \forall\ l \in \mathcal{L}.$$

This condition implies that the inelastic flows are supportable by the network, i.e., there exists a rate division of the inelastic flow rates over their available routes that can support the arriving traffic.

Assumption 3: The utility functions $\{U_\mathrm{e}(x_\mathrm{e})\}_{f_\mathrm{e}}$ are strictly concave, twice differentiable, and increasing functions. Such an assumption is commonly used to capture the diminishing returns to the elastic flows of an increase in the service rate.

[1]We note that the rate controller with source reservoir as in [21] that considers arbitrary load scenario can be added on top of our algorithm.

IEEE Proof Print Version

Assumption 4: For each elastic flow $f_{\rm e} \in \mathcal{F}_{\rm e}$, its utility function $U_{\rm e}(x)$ satisfies the following: For each $m > 0$ and $M \in [m, \infty)$, there exists $\tilde{c}_1$, $\tilde{C}_1$, $\tilde{c}_2$, and $\tilde{C}_2$, with $0 < \tilde{c}_1 < \tilde{C}_1 < +\infty, 0 < \tilde{c}_2 < \tilde{C}_2 < +\infty$, satisfying $\tilde{c}_1 \leq U''_{\rm e}(x) \leq \tilde{C}_1$, $\tilde{c}_2 \leq \left(U'^{-1}_{\rm e}\right)'(x) \leq \tilde{C}_2$, for all $x \in [m, M]$.

We note that Assumption 1 is not critical in the proof of stability, but will simplify our proof, and we will eventually relax the single-route constraint on the elastic flows in Section IV-B. Also note that Assumptions 3 and 4 on the utility functions are not restrictive and hold for the following class of utility functions $U(x) = w > x^{(1-a)}/(1-a)$, for $a > 0$, which is known to characterize a large class of fairness concepts such as max-min fairness and weighted-proportional fairness (see [26] and the references therein).

In subsequent discussions, when the distinction between real and nonreal-time routes is unnecessary, we will simply refer to a route as $\mathbf{R}$ without any subscripts. Furthermore, for simplicity, we will use $z_l[t]$ for $z_l(\mathbf{x}_{\rm i}[t])$ and $y_l[t]$ for $y_l(\mathbf{x}_{\rm e}[t])$.

Queueing Architecture and Evolution: In our system, for each link $(i,j) \in \mathcal{L}$, a single-priority queue is maintained at the transmitting node i, which holds all the packets whose routes traverse (i,j). Since the inelastic flows are expected to have more stringent delay constraints, their packets are always stored ahead of those of the elastic flows, giving inelastic traffic full priority over its elastic counterpart. We let $p_l[t]$ denote the queue length of the buffer associated with link l at the beginning of slot t, and define

$$q_{\mathbf{R}}[t] = \sum_{l \in \mathcal{L}} \mathbf{R}[l] p_l[t]$$

to be the total queue length on route $\mathbf{R}$. Notice that $p_l[t]$ and $q_{\mathbf{R}}[t]$ counts both the inelastic and elastic flows' packets.

During each time slot, the queue p_l evolves as

$$p_l[t+1] = (p_l[t] + y_l[t] + z_l[t] - c_l)^+ \tag{1}$$

where $x^+ = \max(0, x)$. This evolution is based on a *link-centric* decomposition ([18]) and implicitly assumes that packets injected into the source nodes by the flows, denoted by $\mathbf{x}[t]$, arrive at the downstream nodes instantaneously. In reality, packets will reach downstream nodes only after a queueing and propagation delay incurred in the intermediate nodes. It is shown in prior works [5], [18], [29], [30] that the inclusion of these dynamics does not affect the long-term stability and fairness characteristics of the system. In particular, a *regulator* queue for each flow can be added to our queueing architecture before the queues associated with each link as the same architecture in [5]. The prioritization in the per-link queue does not affect the queue evolution, hence the results in [5] apply in our model with priority. Thus, in this work we use the evolution in (1), which possesses a more tractable and cleaner form.

Definition 1 (Stability): We say that a queue $q_{\mathbf{R}}$ is *stable* if

$$\limsup_{T \to \infty} \frac{1}{T} \sum_{t=0}^{T-1} \mathbb{E}(q_{\mathbf{R}}[t]) \leq B \tag{2}$$

where B is some finite positive value. We say that the *network is stable* if all aggregate queues $\{q_{\mathbf{R}}\}$ for both inelastic and elastic flows are stable.

Given this network and traffic model, we aim to do the following.

- Develop a mechanism that maximizes the total utility achieved by elastic flows while giving strict priority to and satisfying the rate demands of the inelastic traffic. To that end, we design a joint congestion control and load-balancing algorithm in Section III.
- Investigate means of extending our mechanism to improve the delay performance of both types of flows. To that end, we extend our joint algorithm in Section IV-A by adding appropriately constructed virtual queues with controllable parameters into the framework to achieve delay improvements.
- By relaxing the single-route constraint (and thus removing Assumption 1) on the elastic flow and adapting a new queueing architecture, we develop a joint congestion control, dynamic routing, and load-balancing algorithm in Section IV-B.

Before addressing these goals, we note that the load-balancing component of our joint algorithm will dynamically control the distribution the inelastic flow rates over its available routes. Thus, the effect of inelastic traffic on the elastic traffic cannot be simply modeled as a constant decrease in the capacity of the network, and a more sophisticated approach is needed. In particular, the inelastic flow rates on each route must be balanced optimally to allow for the maximum utilization of the network resources by the competing elastic flows. We develop such an algorithm in Section III.

III. Joint Congestion Control and Load Balancing

In this section, we address our first main objective, i.e., that of developing an algorithm that provides maximum utilization of elastic traffic while guaranteeing the support of inelastic traffic. We start by describing our objective mathematically in the form of a stochastic optimization problem.

Stochastic Network Optimization (SNO) Problem:

$$\begin{aligned} \max_{\{\mathbf{x}[t] \geq 0\}_{t \geq 0}} \quad & \sum_{f_{\rm e} \in \mathcal{F}_{\rm e}} U_{\rm e}(\bar{x}_{\rm e}) \\ s.t. \quad & \text{Queue Evolution as in } (1) \\ & \text{Network Stability as in } (2) \\ & \sum_{r=1}^{|\mathcal{R}_{\rm i}|} x_{\rm i}^{(r)}[t] = A_{\rm i}[t] \qquad \forall\, f_{\rm i} \in \mathcal{F}_{\rm i} \quad \forall\, t > 0. \end{aligned} \tag{3}$$

We solve this problem by first analyzing a simpler deterministic fluid model in Section III-A. The solution to this fluid model will help in exposition as well as in providing insights on the solution of the above more complex problem. Then, we return in Section III-B to the stochastic problem.

A. Heuristic Fluid Model

In the fluid model scenario, all the dynamics and randomness are ignored, and the stochastic constraints are replaced with static constraints. In particular, the inelastic flow $f_{\rm i}$ is assumed to have a fixed arrival rate $a_{\rm i}$, and the network stability condition is replaced by a condition on total link rate being no more

IEEE Proof Print Version

than capacity. Then, the SNO problem reduces to the following problem in this scenario.

Fluid Network Optimization (FNO) Problem:

$$\max_{\mathbf{x}\geq 0} \quad \sum_{f_{\rm e}\in\mathcal{F}_{\rm e}} U_{\rm e}(x_{\rm e})$$
$$s.t. \quad y_l(\mathbf{x}_{\rm e}) + z_l(\mathbf{x}_{\rm i}) \leq c_l \qquad \forall\, l\in\mathcal{L} \tag{4}$$
$$\sum_{r=1}^{|\mathcal{R}_{\rm i}|} x_{\rm i}^{(r)} = a_{\rm i} \qquad \forall\, f_{\rm i}\in\mathcal{F}_{\rm i}. \tag{5}$$

In our discussion, we will abbreviate the aggregate elastic and inelastic rates, $y_l(\mathbf{x}_{\rm e})$ and $z_l(\mathbf{x}_{\rm i})$, with y_l and z_l for brevity. We note that condition (4) aims to capture the network stability condition in the fluid model by guaranteeing that the total load on a link is below the link capacity, and condition (5) guarantees that inelastic flows receive enough bandwidth to satisfy its rate demands. Thus, the optimization problem is to maximize the sum of utilities of elastic flows when guaranteeing that inelastic flows are supported.

It is not difficult to show that the optimum value of FNO is an upper bound for the optimum value of SNO. To see this, note that any solution $\{\mathbf{x}[t]\}_{t\geq 0}$ that solves SNO must also satisfy $\bar{y}_l + \bar{z}_l \leq c_l$, where $\bar{y}_l := \lim_{T\to\infty}\frac{1}{T}\sum_{t=0}^{T-1} y_l(\mathbf{x}[t])$, and $\bar{z}_l$ is defined similarly. Otherwise, the queue l cannot be stable. This is equivalent to condition (4) in FNO. Thus, FNO contains all the feasible points of SNO. In Section III-B, we will design an algorithm under which SNO can get arbitrarily close to the FNO solution, and thus guarantees the optimality of SNO.

We start by showing that there exists a unique $\mathbf{x}_{\rm e} = \{x_{\rm e}\}_{f_{\rm e}\in\mathcal{F}_{\rm e}}$ that solves the FNO problem under Assumptions 2 and 3.[2]

Proposition 1: If Assumptions 2 and 3 hold, then the $\mathbf{x}_{\rm e}^* = \{x_{\rm e}\}_{f_{\rm e}\in\mathcal{F}_{\rm e}}$ that solves the network optimization problem is unique.

Proof: The optimization problem has a unique solution because the utility functions are strictly concave, and constraints (4) and (5) are linear. ∎

To solve the FNO problem, we construct a partial Lagrangian. Define α_l to be the Lagrange multipliers associated with constraint (4). Then, the partial Lagrangian can be written as

$$\begin{aligned} L(\mathbf{x}_{\rm i},\mathbf{x}_{\rm e},\alpha) &= \sum_{f_{\rm e}\in\mathcal{F}_{\rm e}} U_{\rm e}(x_{\rm e}) - \sum_{l\in\mathcal{L}}\alpha_l(z_l+y_l-c_l) \\ &= \sum_{f_{\rm e}\in\mathcal{F}_{\rm e}}\left(U_{\rm e}(x_{\rm e}) - \left(\sum_{l:\mathbf{R}_{\rm e}^{(r)}[l]=1}\alpha_l\right)x_{\rm e}\right) \\ &\quad + \sum_{l\in\mathcal{L}}\alpha_l(c_l-z_l). \end{aligned}$$

Since the FNO problem satisfies Slater's condition [4] due to Assumption 2, the strong duality holds. We can then conclude that there exists $\mathbf{x}^* := (\mathbf{x}_{\rm e}^*, \mathbf{x}_{\rm i}^*)$, and $\alpha^* := (\alpha_l)_l$ such that:

- $\mathbf{x}^*$ solves the FNO problem;
- $\mathbf{x}^* \in \arg\max_{\mathbf{x}\geq 0} L(\mathbf{x}_{\rm i},\mathbf{x}_{\rm e},\alpha^*)$.

[2]We note that the strict concavity assumption in Assumption 3 can be relaxed, and our results can be extended to state that the elastic rates converge to the *set* of optimal rates rather than the *unique* optimum rate.

Note that

$$\begin{aligned} \max L(\mathbf{x},\alpha^*) = \max \sum_{f_{\rm e}\in\mathcal{F}_{\rm e}} &\left(U_{\rm e}(x_{\rm e}) - \beta^*_{\mathbf{R}_{\rm e}} x_{\rm e}\right) \\ &- \min\sum_{l\in\mathcal{L}}\alpha_l^* z_l + \sum_{l\in\mathcal{L}}\alpha_l^* c_l \end{aligned}$$

where $\beta_{\mathbf{R}} := \sum_{l\in\mathcal{L}}\mathbf{R}[l]\alpha_l$. This decomposition suggests the following conditions.

(i) The elastic flow $f_{\rm e}$ should allocate its rates such that

$$x_{\rm e}^* = U_{\rm e}'^{-1}\left(\beta^*_{\mathbf{R}_{\rm e}}\right). \tag{6}$$

(ii) The inelastic flow $f_{\rm i}$ should distribute its packets over its available routes $\left\{x_{\rm i}^{*(r)}\right\}_{r\in\mathcal{R}_{\rm i}}$ such that

$$\begin{aligned} \min \quad & \sum_{r=1}^{|\mathcal{R}_{\rm i}|} x_{\rm i}^{(r)}\beta^*_{\mathbf{R}_{\rm i}^{(r)}} \\ s.t. \quad & \sum x_{\rm i}^{(r)} = a_{\rm i}. \end{aligned} \tag{7}$$

Since the optimization problem (7) has a linear objective, the following lemma holds [4].

Lemma 1: For any $\mathbf{R}_{\rm i}^{(r)} \in \mathcal{R}_{\rm i}$, we have:

- $\beta^*_{\mathbf{R}_{\rm i}^{(r)}} = \beta^*_{\mathbf{R}_{\rm i}^{(r')}}$ if $x_{\rm i}^{*(r)} > 0$ and $x_{\rm i}^{*(r')} > 0$;
- $\beta^*_{\mathbf{R}_{\rm i}^{(r)}} < \beta^*_{\mathbf{R}_{\rm i}^{(r')}}$ if $x_{\rm i}^{*(r)} > 0$ and $x_{\rm i}^{*(r')} = 0$.

This lemma implies that considering an inelastic flow $f_{\rm i}$, all routes in the optimal solution with a positive flow have the same value of β.

We note that α_l of FNO is closely associated with the queue length p_l of SNO, and correspondingly $\beta_{\mathbf{R}}$ of FNO is closely associated with the aggregate queue length on a route $q_{\mathbf{R}}$ of SNO. Such connections are revealed and exploited in several earlier works for designing different network algorithms (e.g., [6], [7], [16], [17], and [27]). The following algorithm is a continuous-time version of the Lagrangian method for finding the optimum solution of FNO. This algorithm will later be used to solve the SNO. To distinguish the continuous-time evolution from the discrete-time evolution, we use (t) to denote continuous-time index, while $[t]$ denotes discrete-time index.

Joint Congestion Control and Load-Balancing Algorithm for the FNO Problem:

- Queue evolution for link l

$$\dot{p}_l(t) := \frac{dp(t)}{dt} = (z_l(t)+y_l(t)-c_l)^+_{p_l(t)}$$

where $(v(t))^+_{p(t)}$ is zero if $v(t)<0$ and $p(t)=0$; and $v(t)$ otherwise.

- Congestion controller for elastic flow $f_{\rm e}$

$$x_{\rm e}(t) = U_{\rm e}'^{-1}(q_{\mathbf{R}_{\rm e}}(t)).$$

- Load balancing implemented for inelastic flow $f_{\rm i}$

$$\dot{x}_{\rm i}^{(r)}(t) = \left(\bar{q}_{\rm i}(t) - q_{\mathbf{R}_{\rm i}^{(r)}}(t)\right)^+_{x_{\rm i}^{(r)}(t)} \tag{8}$$

IEEE Proof Print Version

where $\bar{q}_{\rm i}(t)$ satisfies

$$\sum_{r=1}^{|\mathcal{R}_{\rm i}|}\left(\bar{q}_{\rm i}(t)-q_{\mathbf{R}_{\rm i}^{(r)}}(t)\right)^{+}_{x_{\rm i}^{(r)}(t)}=0 \tag{9}$$

and $\sum_{r=1}^{|\mathcal{R}_{\rm i}|}x_{\rm i}^{(r)}(0)=a_{\rm i}$.

Remark: Note that the congestion control algorithm is motivated by equality (6). The load-balancing algorithm (8) is motivated by Lemma 1. In particular, for each inelastic flow $f_{\rm i}$, when the system reaches the equilibrium, we have $\dot{x}_{\rm i}^{(r)}(t)=0$ for all r. This implies that $q_{\mathbf{R}_{\rm i}^{(r)}}(t)=\bar{q}_{\rm i}(t)$ for $x_{\rm i}^{(r)}(t)>0$ and $q_{\mathbf{R}_{\rm i}^{(r)}}(t)\geq\bar{q}_{\rm i}$ for $x_{\rm i}^{(r)}(t)=0$. Thus, at the equilibrium point, $q_{\mathbf{R}_{\rm i}^{(r)}}(t)$ satisfies Lemma 1. Furthermore, from (9), it is easy to see that

$$\sum_{r=1}^{|\mathcal{R}_{\rm i}|}x_{\rm i}^{(r)}(t)=a_{\rm i},\qquad\text{for all } t. \tag{10}$$

The intuition behind the load-balancing algorithm described above is to shift the inelastic flows to less heavily loaded routes to allow for the maximum network utilization for elastic flows. In the algorithm, a source needs all the queue information along its route. However, as we mentioned in Section II, we can send queue information hop by hop and still achieve stability even if this information is delayed. Thus, this algorithm can be implemented fully distributed.

Next, we will show the stability and optimality of our joint congestion control and load-balancing algorithm.

Proposition 2: Under Assumptions 1–3, the joint congestion control and load-balancing algorithm is globally asymptotically stable, i.e., $\lim_{t\to\infty}(\mathbf{x}_{\rm e}(t),\mathbf{x}_{\rm i}(t),\mathbf{p}(t),\mathbf{q}(t))=(\mathbf{x}_{\rm e}^*,\mathbf{x}_{\rm i}^*,\alpha^*,\beta^*)$, where $(\mathbf{x}_{\rm e}^*,\mathbf{x}_{\rm i}^*,\alpha^*,\beta^*)$ is an optimal prime-dual solution to the FNO problem. Furthermore, (10) holds.

Proof: The proof is provided in Appendix A. ∎

B. Stochastic Model

We now return to the original SNO problem with a minor variation.

SNO Problem with Parameter *K* (SNO-K):

$$\begin{aligned}\max_{\{\mathbf{x}[t]\geq 0\}_{t\geq 0}}\quad & \sum_{f_{\rm e}\in\mathcal{F}_{\rm e}}KU_{\rm e}(\bar{x}_{\rm e})\\ s.t.\quad & \text{Queue Evolution as in (1)}\\ & \text{Network Stability as in (2)}\\ & \sum_{r=1}^{|\mathcal{R}_{\rm i}|}x_{\rm i}^{(r)}[t]=A_{\rm i}[t]\qquad\forall\, f_{\rm i}\in\mathcal{F}_{\rm i}\quad\forall\, t>0\end{aligned}$$

where K is a positive design parameter. We will see that K-parameter is critical in eliminating the effect of randomness in the stochastic system on the long-term performance. Note that the solution to the SNO-K problem is independent of the value of K, and its optimum solution is identical to the solution of the SNO problem.

Motivated by the analysis in the fluid model, we propose the following joint congestion control and load-balancing algorithm.

Joint Congestion Control and Load-Balancing Algorithm for the SNO-K Problem:

- Scheduling with Strict Prioritization:
  For each link $l\in\mathcal{L}$, we serve c_l packets from p_l, with strict priority to inelastic packets, which leads to the following queue evolution:
  $$p_l[t+1]=(p_l[t]+z_l[t]+y_l[t]-c_l)^{+}.$$
- Congestion controller for elastic flow $f_{\rm e}$
  $$x_{\rm e}[t]=\min\left\{M,U_{\rm e}'^{-1}\left(\frac{1}{K}q_{\mathbf{R}_{\rm e}}[t]\right)\right\}$$
  where M is a positive constant satisfies $M>2\max_{l\in\mathcal{L}}\{c_l\}$.
- Load balancing implemented for inelastic flow $f_{\rm i}$
  $$\triangle x_{\rm i}^{(r)}[t]=\left(\bar{q}_{\rm i}[t]-q_{\mathbf{R}_{\rm i}^{(r)}}[t]\right)^{+}_{x_{\rm i}^{(r)}[t+1]}$$
  or equivalently
  $$x_{\rm i}^{(r)}[t+1]=\left(x_{\rm i}^{(r)}[t]+\bar{q}_{\rm i}[t]-q_{\mathbf{R}_{\rm i}^{(r)}}[t]\right)^{+}$$
  where $\bar{q}_{\rm i}[t]$ satisfies
  $$\sum_{r=1}^{|\mathcal{R}_{\rm i}|}\left(\bar{q}_{\rm i}[t]-q_{\mathbf{R}_{\rm i}^{(r)}}[t]\right)^{+}_{x_{\rm i}^{(r)}[t+1]}=A_{\rm i}[t+1]-A_{\rm i}[t]$$
  and $\sum_{r=1}^{|\mathcal{R}_{\rm i}|}x_{\rm i}^{(r)}[0]=A_{\rm i}[0]$.

Remark: The factor $1/K$ in the congestion control equation comes from the factor K in the optimization problem. It can be interpreted as the aggressiveness factor of the elastic flow, as the congestion controller is inclined to inject more packets into the network with larger K. Also note that the load-balancing implementation is slightly different from the fluid model version to accommodate the randomness in the arrival processes for inelastic flows. The update is modified to ensure that $\sum_{r=1}^{|\mathcal{R}_{\rm i}|}x_{\rm i}^{(r)}[t]=A_{\rm i}[t]$ holds for all t.

The next proposition establishes the stability and optimality of the joint algorithm for the stochastic system.

Proposition 3: Under Assumptions 1–4, the joint congestion control and load-balancing algorithm stabilizes the system in the sense that the Markov chain $(\mathbf{p}[t],\mathbf{x}_{\rm i}[t])$ is positive recurrent with

$$\limsup_{T\to\infty}\frac{1}{T}\sum_{t=0}^{T-1}\mathbb{E}\left(\left\|\mathbf{q}_{\mathbf{R}_{\rm e}}[t]-\beta_{\mathbf{R}_{\rm e}}^*\right\|\right)\leq\frac{B+\epsilon\sigma K}{\epsilon}$$

and guarantees that the rate allocation satisfies

$$\limsup_{T\to\infty}\frac{1}{T}\sum_{t=0}^{T-1}\mathbb{E}\left(\|\mathbf{x}_{\rm e}[t]-\mathbf{x}_{\rm e}^*\|^2\right)\leq\frac{B}{\tilde{c}_3K}.$$

IEEE Proof Print Version

Here, $\mathbf{x}_{\mathrm{e}}^*$ is the optimal solution to the SNO-K problem, σ is an arbitrarily chosen positive constant, and ϵ and $\tilde{c}_3$ are positive values. ■

Proof: See [15] for the proof. ■

Note that as the design parameter K increases, the rate converges to the optimal allocation at the cost of increased equilibrium queue-length levels. While such tradeoffs between optimality and delay are observed in earlier works under a single type of traffic (e.g., [7] and [21]), in this work a new interaction is observed between inelastic and elastic traffic through the parameter K. In particular, larger values of K result in more aggressive elastic flows, resulting in larger queue lengths on the links they traverse. This forces the inelastic flows to redistribute their flows to less loaded routes. This increases the utilization of the network, while causing more delay to inelastic flows. In order to provide better delay performance to both types of traffic, in the next section we extend our base algorithm by using virtual queues.

IV. Extension of the Algorithm

In this section, we extend our joint congestion control and load-balancing algorithm in two important directions. We first provide a virtual queue-based solution that reduces the overall queue length with a negligible sacrifice in capacity. We then provide a solution that allows the dynamic routing for the elastic flow.

A. Virtual Queue Algorithm

Inelastic applications are delay-sensitive, hence we assume that packets from inelastic flows have strict priority over their elastic counterparts. Thus, the inelastic flows do not see the elastic flows in the queues they traverse. However, in some cases a link might be critically loaded by the inelastic traffic itself, thus resulting in large delays. Also, elastic traffic may have some delay constraints that are nonnegligible.

An effective way of reducing the experienced delay is by including virtual queues that are served at a fraction of the actual service rate and by using the virtual queue-length values as prices [13]. To that end, we introduce two types of virtual queues with parameters to the previous optimization problem, ρ_1 and ρ_2, which control the total load and the inelastic flow load, respectively.

Here for simplicity, we go back to the fluid model to design and analyze the joint congestion control and load-balancing algorithm using virtual queues. We would like to have $\tilde{\mathbf{x}}^* := (\tilde{\mathbf{x}}_{\mathrm{e}}^*, \tilde{\mathbf{x}}_{\mathrm{i}}^*)$ solve the following optimization problem.

FNO Problem With Virtual Queues (FNO-VQ):

$$\begin{aligned} \max_{\mathbf{x}\geq 0} \quad & \sum_{f_{\mathrm{e}}\in\mathcal{F}_{\mathrm{e}}} U_{\mathrm{e}}(x_{\mathrm{e}}) \\ s.t. \quad & y_l(\mathbf{x}_{\mathrm{e}}) + z_l(\mathbf{x}_{\mathrm{i}}) \leq \rho_1 c_l \qquad \forall\, l \in \mathcal{L} \\ & z_l(\mathbf{x}_{\mathrm{i}}) \leq \rho_2 c_l \qquad \forall\, l \in \mathcal{L} \\ & \sum_{r=1}^{|\mathcal{R}_{\mathrm{i}}|} x_{\mathrm{i}}^{(r)} = a_{\mathrm{i}} \end{aligned} \tag{11}$$

where $0 < \rho_2 \leq \rho_1 < 1$.

To guarantee the feasibility of this optimization problem, we replace our earlier Assumption 2 with Assumption 5.

Assumption 5: There exists an $\mathbf{x}_{\mathbf{i}}$ such that

$$\sum_{r=1}^{|\mathcal{R}_{\mathrm{i}}|} x_{\mathrm{i}}^{(r)} = a_{\mathrm{i}} \;\forall\, f_{\mathrm{i}} \in \mathcal{F}_{\mathrm{i}} \quad \text{and} \quad z_l(\mathbf{x}_{\mathbf{i}}) < \rho_2 c_l \;\forall\, l \in \mathcal{L}.$$

This can be viewed as admission control is done for the inelastic flow after we choose the parameter ρ_2 to ensure the feasibility of the problem.

To solve the FNO-VQ problem, we first introduce virtual queues for elastic and inelastic flows on each link, respectively. The virtual queue length $\theta_l(t)$ for elastic flows evolves as follows:

$$\dot{\theta}_l(t) = (z_l(t) + y_l(t) - \rho_1 c_l)^+_{\theta_l(t)}.$$

The virtual queue length for inelastic flows $\gamma_l(t)$ evolves as follows:

$$\dot{\gamma}_l(t) = (z_l(t) - \rho_2 c_l)^+_{\gamma_l(t)}.$$

Note that when the total instantaneous traffic load is larger than $\rho_1 c_l$ or the inelastic traffic load is larger than $\rho_2 c_l$, the virtual queues will build up, and the network controller will reduce the traffic load.

Based on this virtual queue scheme, we have the following joint congestion control and load-balancing algorithm.

Joint Congestion Control and Load-Balancing Algorithm for FNO-VQ Problem:

- Virtual queue evolution for a link l

$$\begin{aligned} \text{Elastic flows:} \quad & \dot{\theta}_l(t) = (z_l(t) + y_l(t) - \rho_1 c_l)^+_{\theta_l(t)} \\ \text{Inelastic flows:} \quad & \dot{\gamma}_l(t) = (z_l(t) - \rho_2 c_l)^+_{\gamma_l(t)}. \end{aligned}$$

- Congestion controller for elastic flow f_{e}

$$x_{\mathrm{e}}(t) = U_{\mathrm{e}}'^{-1}(s_{\mathbf{R}_{\mathrm{e}}}(t))$$

where $s_{\mathbf{R}_{\mathrm{e}}}(t) = \sum_{l:\mathbf{R}_{\mathrm{e}}[l]=1} \theta_l(t)$ is the aggregated virtual queue length of the elastic flow.

- Load balancing implemented for inelastic flow f_{i}

$$\dot{x}_{\mathrm{i}}^{(r)}(t) = \left(\bar{\mu}_{\mathrm{i}}(t) - \mu_{\mathbf{R}_{\mathrm{i}}^{(r)}}(t)\right)^+_{x_{\mathrm{i}}^{(r)}(t)}$$

where $\mu_{\mathbf{R}}(t) = \sum_{l:\mathbf{R}[l]=1}(\theta_l(t) + \gamma_l(t))$, $\bar{\mu}_{\mathrm{i}}(t)$ satisfies

$$\sum_{r=1}^{|\mathcal{R}_{\mathrm{i}}|} \left(\bar{\mu}_{\mathrm{i}}(t) - \mu_{\mathbf{R}_{\mathrm{i}}^{(r)}}(t)\right)^+_{x_{\mathrm{i}}^{(r)}(t)} = 0$$

and $\sum_{r=1}^{|\mathcal{R}_{\mathrm{i}}|} x_{\mathrm{i}}^{(r)}(0) = a_i$.

Remark: In the above algorithm, note that the congestion control algorithm only responds to the virtual queues for elastic flows, but the load-balancing algorithm responds to both the virtual queues for elastic flows and inelastic flows. Furthermore, the actual queue length is not used in the algorithm.

IEEE Proof Print Version

In the following proposition, we show the equilibrium point of the algorithm with virtual queue is the optimal solution of (11).

Proposition 4: Under Assumptions 1, 3, and 5, the virtual system under the joint congestion control and load-balancing algorithm for the FNO-VQ problem is globally asymptotically stable, i.e., $\lim_{t\to\infty}(\mathbf{x}_{\rm e}(t),\mathbf{x}_{\rm i}(t),\theta(t),\gamma(t)) = \left(\tilde{\mathbf{x}}_{\rm e}^*,\tilde{\mathbf{x}}_{\rm i}^*,\tilde{\theta}^*,\tilde{\gamma}^*\right)$, where $\left(\tilde{\mathbf{x}}_{\rm e}^*,\tilde{\mathbf{x}}_{\rm i}^*,\tilde{\theta}^*,\tilde{\gamma}^*\right)$ is an optimal primal-dual solution of the network optimization problem (11). ■

Proof: See [15] for the proof. ■

Remark: Proposition 4 implies the stability of the virtual system. Since the virtual system is run in a network with smaller link capacity, it is intuitively reasonable to expect the real queue lengths be stable. While this intuition is confirmed in numerical studies, we do not claim the stability of the real system under this algorithm.

The extension of this result to the stochastic scenario is omitted since it follows the same line of reasoning as in the joint congestion control and load-balancing algorithm of Section III.

B. Dynamic Routing for Elastic Flows

Here, we keep the assumptions of the inelastic flows and relax the single-route constraint on the elastic flows. Each elastic flow $f_{\rm e} = f_s^d$ now is associated with a source node $s \in \mathcal{N}$ and a destination node $d \in \mathcal{N}$. The injection rate of the flow f_s^d is denoted by x_s^d, and $U_s^d\left(x_s^d\right)$ is the utility function.

In this model, we adapt a new queueing architecture. Each node i maintains both real queues and virtual queues (counters), which are identical structural-wise. We focus on the virtual queues, which are neater to analyze.

Within the virtual queues, there are two levels of queues. The first level of the virtual queues are for each destination for elastic flows, denoted by $s_i^d[t]$, each node maintains $|\mathcal{N}|-1$ such queues. Let $r_{ij}^d[t]$ denote the promised service rate to elastic flows that are destined to d on link $l=(i,j)$, and let

$$y_l[t] = \sum_{d\in\mathcal{N}} r_{ij}^d[t]$$

denotes the total promised service of elastic flows on link l. These counters evolve as

$$s_i^d[t+1] = \left(s_i^d[t] + x_i^d[t] + \sum_{m\in\mathcal{N}} r_{mi}^d[t] - \sum_{j\in\mathcal{N}} r_{ij}^d[t]\right)^+. \tag{12}$$

The second level of virtual queues consists of a virtual queue for each outgoing link, denoted by $p_{ij}[t]$ where $(i,j)\in\mathcal{L}$, which counts packets from both inelastic and elastic flows. Packets of the inelastic flows are always "stored" ahead of those of the elastic flows. These counters evolve as

$$p_l[t+1] = (p_l[t] + y_l[t] + z_l[t] - c_l)^+. \tag{13}$$

Remark 1: Note that in the virtual queues (counters), $r_{ij}^d[t]$ virtual packets "bypass" the queueing in the second level of virtual queues and directly enter the corresponding first-level virtual queues of the next node, while $r_{ij}^d[t]$ actual packets are forwarded within the node to the second level of queues, waiting to be transmitted onto the corresponding link to the downstream node. The decisions made by the algorithm are based on the virtual queue information, which is a "prediction" of the actual queue lengths. We will see that the actual queues evolve in the same way when the system reaches its equilibrium point.

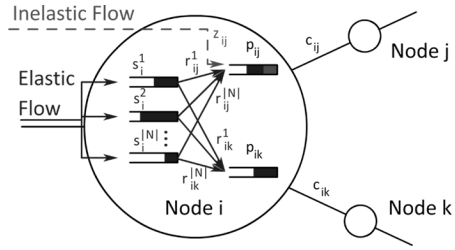

Fig. 1. Queueing architecture for dynamic routing.

Remark 2: The evolution of $p[t]$ given in (13) implicitly assumes that the inelastic packets injected into the source nodes arrive at the downstream nodes immediately. Prior works [5], [18], [29], [30] show that this assumption does not affect the long-term performance of the system. Since the inelastic traffic enters the second-level queues directly, the results of those works still apply to the inelastic flows. In particular, a regulator queue for each inelastic flow can be added to our queueing architecture before the second-level queues associated with each link following the same approach as in [5].

The queueing architecture described is illustrated in Fig. 1.

For simplicity, we consider the fluid model scenario for dynamic routing.

FNO Problem With Dynamic Routing (FNO-DR):

$$\max_{\mathbf{x}\geq 0} \quad \sum_{f_{\rm e}\in\mathcal{F}_{\rm e}} U_{\rm e}(x_{\rm e}) \tag{14}$$

$$s.t. \quad y_l(\mathbf{r}) + z_l(\mathbf{x}_i) \leq c_l \qquad \forall\, l\in\mathcal{L} \tag{15}$$

$$\sum_{r=1}^{|\mathcal{R}_{\rm i}|} x_{\rm i}^{(r)} = a_{\rm i} \qquad \forall\, f_{\rm i}\in\mathcal{F}_{\rm i} \tag{16}$$

$$x_{\rm i}^d + \sum_{m\in\mathcal{N}} r_{mi}^d \leq \sum_{j\in\mathcal{N}} r_{ij}^d \qquad \forall\, i,d\in\mathcal{N}, i\neq d \tag{17}$$

$$r_{ij}^d \leq P \qquad \forall\,(i,j)\in\mathcal{L}, d\in\mathcal{N} \tag{18}$$

where (17) is the flow conservation constraint, and (18) is a fixed bound on r_{ij}^d, where $P \geq \max_{l\in\mathcal{L}}\{c_l\}$.

Based on the new queueing architecture and the FNO-DR problem, using the Lagrange multiplier approach, we have the following joint congestion control, dynamic routing, and load-balancing algorithm.

Joint Congestion Control, Dynamic Routing, and Load-Balancing Algorithm for the FNO-DR Problem:

- Virtual queue evolution

$$\dot{s}_i^d(t) = \left(x_i^d(t) + \sum_{m\in\mathcal{N}} r_{mi}^d(t) - \sum_{j\in\mathcal{N}} r_{ij}^d(t)\right)^+_{s_i^d(t)}$$

IEEE Proof Print Version

$$\dot{p}_l(t) = (z_l(t) + y_l(t) - c_l)^+_{p_l(t)}.$$

- Congestion controller for elastic flow f_s^d

$$x_s^d(t) = \left(U_s^d\right)'^{-1}\left(s_s^d(t)\right).$$

- Dynamic routing for elastic flow

$$\dot{r}_{ij}^d(t) = \begin{cases} s_i^d(t) - s_j^d(t) - p_{ij}(t), & \text{if } r_{ij}^d \in (0, P) \\ \left(s_i^d(t) - s_j^d(t) - p_{ij}(t)\right)^+, & \text{if } r_{ij}^d \le 0 \\ \left(s_i^d(t) - s_j^d(t) - p_{ij}(t)\right)^-, & \text{if } r_{ij}^d \ge P. \end{cases}$$

- Load balancing for inelastic flow f_{i}

$$\dot{x}_{\mathrm{i}}^{(r)}(t) = \left(\bar{q}_{\mathrm{i}}(t) - q_{\mathbf{R}_{\mathrm{i}}^{(r)}}(t)\right)^+_{x_{\mathrm{i}}^{(r)}(t)}$$

where $q_{\mathbf{R}_{\mathrm{i}}^{(r)}}(t) = \sum_{l\in\mathcal{L}} \mathbf{R}_{\mathrm{i}}[l] p_l(t)$, and $\bar{q}_{\mathrm{i}}(t)$ satisfies

$$\sum_{r=1}^{|\mathcal{R}_{\mathrm{i}}|} \left(\bar{q}_{\mathrm{i}}(t) - q_{\mathbf{R}_{\mathrm{i}}^{(r)}}(t)\right)^+_{x_{\mathrm{i}}^{(r)}(t)} = 0$$

and $\sum_{r=1}^{|\mathcal{R}_{\mathrm{i}}|} x_{\mathrm{i}}^{(r)}(0) = a_i$.

Remark: In the algorithm above, the rate control of the elastic traffic only needs the virtual queue information of the source node, while the load balancing of the inelastic uses the virtual queue information on the whole route. The dynamic routing algorithm for elastic traffic is similar to the back-pressure algorithm, while the backlog difference between the two nodes of a link $s_i^d - s_j^d$ is offset by p_{ij}, discouraging the elastic flows from using the links that are in the route of the inelastic flows. Also, we note that this back-pressure-like algorithm is applied to the elastic traffic only, and the strict priority of the inelastic traffic is still maintained.

In the following proposition, we show the equilibrium point of the algorithm for dynamic routing is the optimal solution of (14).

Proposition 5: Under Assumptions 2 and 3, the virtual system under the joint congestion control, dynamic routing, and load-balancing algorithm for the FNO-DR problem is globally asymptotically stable, i.e., $\lim_{t\to\infty}(\mathbf{x}_{\mathrm{e}}(t), \mathbf{x}_{\mathrm{i}}(t), \mathbf{p}(t), \mathbf{s}(t)) = (\hat{\mathbf{x}}_{\mathrm{e}}^*, \hat{\mathbf{x}}_{\mathrm{i}}^*, \hat{\mathbf{p}}^*, \hat{\mathbf{s}}^*)$ where $(\hat{\mathbf{x}}_{\mathrm{e}}^*, \hat{\mathbf{x}}_{\mathrm{i}}^*, \hat{\mathbf{p}}^*, \hat{\mathbf{s}}^*)$ is an optimal primal-dual solution of the network optimization problem (14).

Proof: The proof is provided in Appendix B. ∎

Remark: Note that the virtual system will evolve to the optimal point according to the equations above, while the actual system may follow a slightly different trajectory. This is because during the transient period of evolution, the total incoming rate of inelastic flow $\mathbf{z}(t)$ and the elastic flow $\mathbf{r}(t)$ into the second level of the queue (cf. Fig. 1) is allowed to be larger than the capacity of the link. Thus, when the system made routing decisions according to the virtual values (the estimated number of packets in the queues), there may not be enough packets to transmit in the actual queues. However, when the virtual system converges to its equilibrium point, the assigned service rate r_{ij}^{*d} will be feasible as shown in Proposition 5, and therefore the actual system will also be able to provide the same rate as the virtual one. Thus, at the equilibrium point, the stability of the virtual system implies the stability of the actual system.

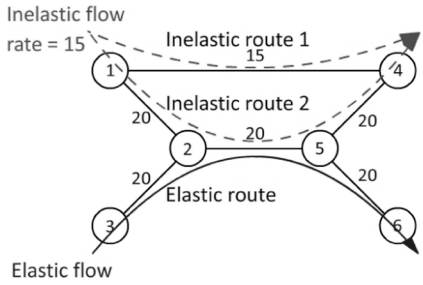

Fig. 2. Topology of the network.

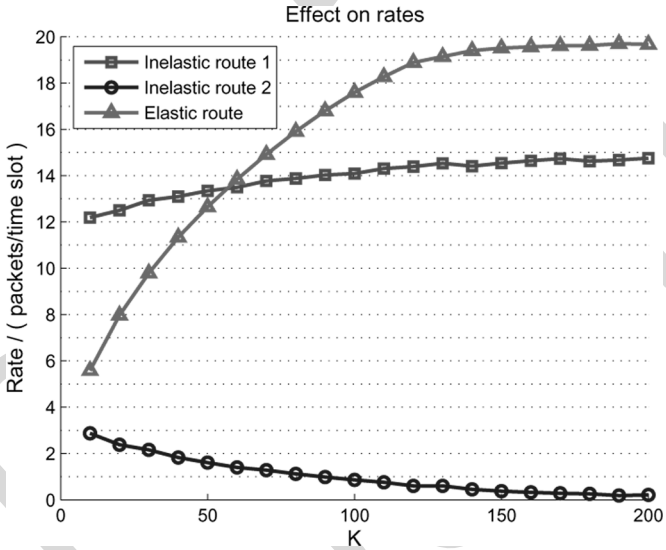

Fig. 3. Effect of K on the average rates on each route of Fig. 2.

V. Simulation Results

In this section, we provide the simulation results for our algorithms under the stochastic model where the arrival process of the inelastic flow f_{i} is such that $A_{\mathrm{i}}[t]$ is Poisson-distributed with mean a_{i} for each t.

A. Effect of the Aggressiveness of the Inelastic Flow

We noted in Section III-B that the factor K represents the "aggressiveness"' of the elastic flows. Also, it is revealed in Proposition 3 that K can be used to control the proximity to the optimal allocation. Here, we test these results for the case of proportionally fair allocation, which corresponds to having the utility function is chosen as [26]: $U_{\mathrm{e}}(x) = \alpha \ln x$, and thus $U_{\mathrm{e}}'^{-1}(\frac{q}{K}) = \frac{\alpha K}{q}$.

In this first set of simulations, we considered the network shown in Fig. 2 with the indicated link capacities and inelastic and elastic flows. Note that the arrival rate of the inelastic flow is $a_{\mathrm{i}} = 15$ to be distributed over the two dashed routes.

The joint algorithm for the SNO-K problem is implemented for this network, and the mean elastic rate allocation is computed for different values of K. Fig. 3 illustrates the effect of K on the rates of the elastic flow and the distribution of the inelastic

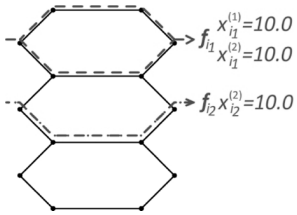

Fig. 4. Phase 1: Two inelastic flows with disjoint routes.

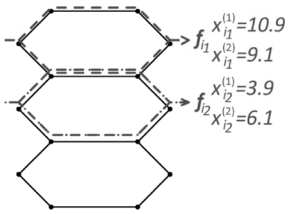

Fig. 5. Phase 2: Two inelastic flows with intersecting routes.

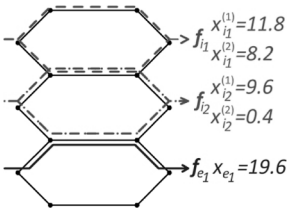

Fig. 6. Phase 3: Two intersecting inelastic flows, and one elastic flow that interacts with them.

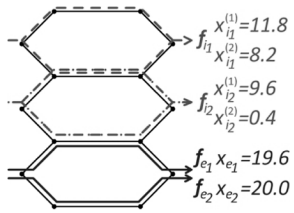

Fig. 7. Phase 4: Two intersecting inelastic flows, and two elastic flows with disjoint routes.

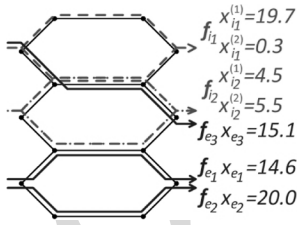

Fig. 8. Phase 5: A third elastic flow enters, which intersects with two inelastic flows.

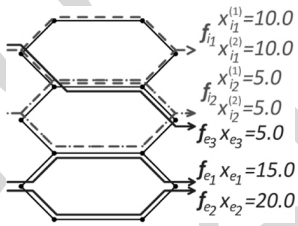

Fig. 9. Performance under static rate distribution for inelastic traffic.

flow's rate over its available routes. We see that as the elastic flow becomes more aggressive, it achieves a higher throughput and thus consumes greater resource on the bottleneck link (2,5). As a reaction to the increased contention from the elastic flow, the load-balancing mechanism of the inelastic flows automatically pushes more and more traffic of the inelastic flow onto route 1.

Note that although increasing the aggressiveness of the elastic flow will increase the utilization of the network, it will result in more delays on the network flows as the queue length over the whole network grows, as shown by Proposition 3. Proposition 3 also suggests that larger K resulting better convergence to the optimal operating point, which is confirmed in the above simulation.

B. More Complex Topology

To illustrate other facets of our algorithm, we conducted our simulation in a more complicated network with different flow assignments. The topology of the network is shown in Fig. 4. The capacity of all the links in the network is 20, and we used elastic flows with identical utility functions and $K = 200$ in our simulation, expecting close-to-optimal utilization (as shown in Fig. 3).

We simulate a sequence of scenarios discussed in five phases. In Phase 1, two disjoint inelastic flows with the routes as shown in Fig. 4 share the network, having rates $a_{\mathrm{i}1} = 20$ and $a_{\mathrm{i}2} = 10$. The average rates provided on each route by our joint algorithm are given in Fig. 4.

When the two inelastic flows share a common bottleneck link in Phase 2, the load-balancing algorithm will shift part of the traffic from the bottleneck link to yield the average rates given in Fig. 5.

In Phase 3, an elastic flow enters the system and shares a link with $f_{\mathrm{i}2}$ as in Fig. 6. We can see from the average rates given in the figure that this elastic flow not only has an effect on $f_{\mathrm{i}2}$, but also shifts the rate of $f_{\mathrm{i}1}$. Here, it can be seen that the interaction between the flows becomes complex even for small networks, and it is not clear what the best allocation is. Yet, through our joint algorithm, $f_{\mathrm{e}1}$ is able to operate dynamically close to the full capacity of all the resources available to it.

After adding another elastic flow $f_{\mathrm{e}2}$ into the network, which is disjoint with all other flows in Phase 4 shown in Fig. 7, we can see that it has no effect on the rates of all other routes, and it fully utilizes that route.

In Phase 5, a third elastic flow $f_{\mathrm{e}3}$ enters and shares common links with both $f_{\mathrm{i}1}$ and $f_{\mathrm{i}2}$, as shown in Fig. 8. We can see that since $f_{\mathrm{e}1}$ also shares links with $f_{\mathrm{i}2}$, $f_{\mathrm{e}3}$ also has effect on it. It can be easily verified that $x_{\mathrm{e}1} = x_{\mathrm{e}3} = 15$ is the optimal operating point, and the average rates achieved by our algorithm are very close to optimal as predicted by Proposition 3.

To study the importance of dynamic load balancing, we also simulated a static rate distribution algorithm as a basis for comparison. This algorithm equally splits the inelastic traffic onto each of its routes (assume it is feasible in the network) and does the congestion control of the elastic flows in the same manner as in our algorithm. This algorithm is implemented for the scenario in Phase 5 with the average rates indicated in Fig. 9. We see that due to the absence of dynamic load balancing, the elastic flows

IEEE Proof Print Version

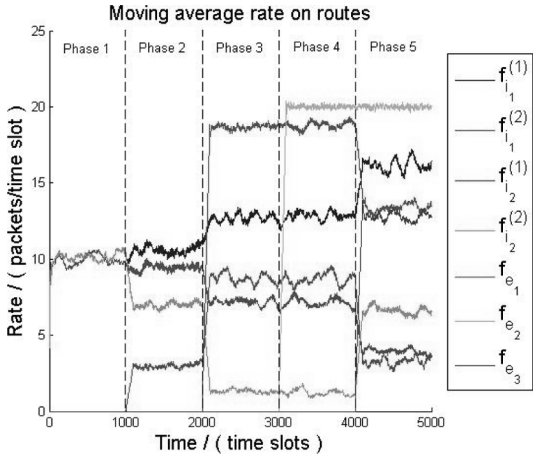

Fig. 10. Injection rate on each route.

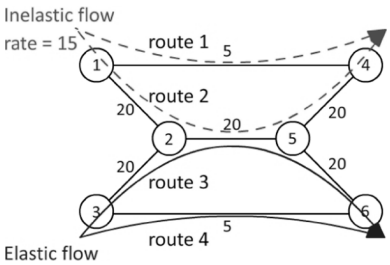

Fig. 11. Network topology for simulating the virtual queue algorithm.

cannot utilize the network fully since the rates assigned to the inelastic flows are fixed. Under the logarithm utility function, this approach achieves a utility of $1.61\alpha K$, while our algorithm achieves $2.71\alpha K$ on the elastic flow $f_{\mathrm{e}3}$.

In this sequence of simulations, we see complex interactions between the elastic and inelastic flows and observed that our algorithm achieves optimal performance distributively. While we have so far focused on the average achieved rates, in Fig. 10, we also show the time evolution of the flow rates on each route as the network goes through the five phases. We see in this figure that the rates converge to their optimal value quickly, which may be important under dynamic conditions.

C. Simulation Using the Virtual Queue Algorithm

In this simulation, we use the joint congestion control and load-balancing algorithm with virtual queue to show the impact of the virtual queue implementation on delay. The simulation is conducted in the network showing in Fig. 11. The parameter ρ_1 was set to 0.95, and ρ_2 was set to 0.9, over all links.

Table I compares the performance with and without virtual queues. First, we note that on link (2,3), though it is critically loaded by two types of flows, the inelastic flow has a much smaller delay compared to the elastic flow due to the strict prioritization. Also, as we can observe, under the original algorithm, route 1 is critically loaded by inelastic flow, resulting in a large delay. With the virtual queue implementation, we manage to decrease the rate on route 1, thus dropping the delay significantly. As one can observe from the table, the delay is greatly

TABLE I
RATE AND DELAY ON EACH ROUTE

	w/o virtual queue		w/ virtual queue	
	rate	delay	rate	delay
route 1	4.9955	40.320	4.4984	0.5405
route 2	9.7414	0.0440	10.502	0.0005
route 3	10.259	15.854	8.5118	1.0137
route 4	4.9950	77.461	4.7817	1.9765

reduced for both elastic and inelastic traffic without a significant degradation in the rate of the elastic traffic. Thus, especially under critical loaded scenarios, virtual queue implementation can achieve significant delay improvements.

Also, for the elastic flows, the delay drops significantly in the tradeoff of a small loss in utilization.

VI. CONCLUSION

In this work, we consider the optimal control of networks that serve heterogeneous traffic types with diverse demands, namely inelastic and elastic traffic. We formulated a new network optimization problem, proposed a novel queueing architecture, and developed a distributed load-balancing and congestion control algorithm with provably optimal performance. We also provided an important improvement to our joint algorithm to achieve better delay performance by introducing new design parameters (ρ_1, ρ_2) together with a set of virtual queues. We have also extended our algorithm to the case of allowing elastic flows to choose their routes dynamically, which will further utilize the resource available in the network.

Future research of this topic includes the following. 1) One future direction is to extend our results to multihop wireless networks with fading channels and interference and develop joint load-balancing/congestion control/routing/scheduling algorithms. 2) Here, we considered a time-slotted system and assumed that the network is perfectly synchronized. The impact of possible asynchronism on the algorithm performance needs to be studied. 3) We adopted a link-centric formulation, which assumes instantaneous arrivals of the packets at all the links on their routes. An alternative is to consider a node-centric formulation, where packets are sequentially transferred, and a source only requires the information of the queues at the source. 4) So far, we have focused on the stability and long-term guarantees for the traffic types. We aim to investigate oscillatory behavior [20] and delay characteristics in our future work. 5) In this work, we assume the routes and the supportability of the inelastic flow are given. Developing corresponding routing and admission control mechanism will make it complete.

APPENDIX A
PROOF OF PROPOSITION 2

Define a Lyapunov function

$$V(\mathbf{p}(t), \mathbf{x}_{\mathrm{i}}(t)) = \frac{1}{2}\sum_{l\in\mathcal{L}} (p_l(t) - \alpha_l^*)^2 + \frac{1}{2}\sum_{f_{\mathrm{i}}\in\mathcal{F}_{\mathrm{i}}}\sum_{r=1}^{|\mathcal{R}_{\mathrm{i}}|}\left(x_{\mathrm{i}}^{(r)}(t) - x_{\mathrm{i}}^{*(r)}\right)^2 \quad (19)$$

IEEE Proof Print Version

where α^* and $\mathbf{x}_{\mathrm{i}}^*$ satisfy conditions (i) and (ii). Note that $\mathbf{x}_{\mathrm{i}}^*$ and α^* may not be unique. Then, we have

$$\begin{aligned}
\frac{d}{dt}V(\mathbf{p}(t),\mathbf{x}_{\mathrm{i}}(t)) &= \sum_{l\in\mathcal{L}}\left(p_l(t)-\alpha_l^*\right)\dot{p}_l(t) \\
&\quad+\sum_{f_i\in\mathcal{F}_{\mathrm{i}}}\sum_{r=1}^{|\mathcal{R}_{\mathrm{i}}|}\left(x_{\mathrm{i}}^{(r)}(t)-x_{\mathrm{i}}^{*(r)}\right)\dot{x}_{\mathrm{i}}^{(r)}(t) \\
&= \sum_{l\in\mathcal{L}}\left(p_l(t)-\alpha_l^*\right)\left(z_l(t)+y_l(t)-c_l\right)_{p_l(t)}^{+} \\
&\quad+\sum_{f_i\in\mathcal{F}_{\mathrm{i}}}\sum_{r=1}^{|\mathcal{R}_{\mathrm{i}}|}\left(x_{\mathrm{i}}^{(r)}(t)-x_{\mathrm{i}}^{*(r)}\right) \\
&\quad\times\left(\bar{q}_{\mathrm{i}}(t)-q_{\mathbf{R}_{\mathrm{i}}^{(r)}}(t)\right)_{x_{\mathrm{i}}^{(r)}(t)}^{+} \\
&\le \sum_{l\in\mathcal{L}}\left(p_l(t)-\alpha_l^*\right)\left(z_l(t)+y_l(t)-c_l\right) \\
&\quad+\sum_{f_i\in\mathcal{F}_{\mathrm{i}}}\sum_{r=1}^{|\mathcal{R}_{\mathrm{i}}|}\left(x_{\mathrm{i}}^{(r)}(t)-x_{\mathrm{i}}^{*(r)}\right) \\
&\quad\times\left(\bar{q}_{\mathrm{i}}(t)-q_{\mathbf{R}_{\mathrm{i}}^{(r)}}(t)\right)_{x_{\mathrm{i}}^{(r)}(t)}^{+} \\
&= \sum_{l\in\mathcal{L}}\left(p_l(t)-\alpha_l^*\right)\left(z_l(t)-z_l^*\right) \\
&\quad+\sum_{l\in\mathcal{L}}\left(p_l(t)-\alpha_l^*\right)\left(y_l(t)+z_l^*-c_l\right) \\
&\quad+\sum_{f_i\in\mathcal{F}_{\mathrm{i}}}\sum_{r=1}^{|\mathcal{R}_{\mathrm{i}}|}\left(x_{\mathrm{i}}^{(r)}(t)-x_{\mathrm{i}}^{*(r)}\right) \\
&\quad\times\left(\bar{q}_{\mathrm{i}}(t)-q_{\mathbf{R}_{\mathrm{i}}^{(r)}}(t)\right)_{x_{\mathrm{i}}^{(r)}(t)}^{+}.
\end{aligned}$$

Next, we show the negativity of the drift term by term. First, we have

$$\begin{aligned}
&\sum_{l\in\mathcal{L}}\left(p_l(t)-\alpha_l^*\right)\left(y_l(t)+z_l^*-c_l\right) \\
&\le \sum_{l\in\mathcal{L}}\left(p_l(t)-\alpha_l^*\right)\left(y_l(t)-y_l^*\right) \\
&= \left(\mathbf{p}^T(t)-\alpha^{*T}\right)\mathbf{R}_{\mathrm{e}}\left(\mathbf{x}_{\mathrm{e}}(t)-\mathbf{x}_{\mathrm{e}}^*\right) \\
&= \left(\mathbf{q}^T(t)-\beta^{*T}\right)\left(\mathbf{x}_{\mathrm{e}}(t)-\mathbf{x}_{\mathrm{e}}^*\right) \\
&= \sum_{f_{\mathrm{e}}\in\mathcal{F}_{\mathrm{e}}}\left(U_{\mathrm{e}}'(x_{\mathrm{e}}(t))-U_{\mathrm{e}}'(x_{\mathrm{e}}^*)\right) \\
&\quad\times\left(x_{\mathrm{e}}(t)-x_{\mathrm{e}}^*\right) \\
&\le 0
\end{aligned} \tag{20}$$

where the first inequality holds because $y_l^*+z_l^*\le c_l$ for any $l\in\mathcal{L}$, and $\alpha_l^*=0$ if $y_l^*+z_l^*<c_l$, $\alpha_l^*>0$ if and only if $y_l^*+z_l^*=c_l$; the second equality holds due to Assumption 1.

Without loss of generality, we assume that $x_{\mathrm{i}}^{*(1)}>0$ for all f_{i}, then we have

$$\begin{aligned}
&\sum_{f_{\mathrm{i}}\in\mathcal{F}_{\mathrm{i}}}\sum_{r=1}^{|\mathcal{R}_{\mathrm{i}}|}\left(x_{\mathrm{i}}^{(r)}(t)-x_{\mathrm{i}}^{*(r)}\right)\left(\bar{q}_{\mathrm{i}}(t)-q_{\mathbf{R}_{\mathrm{i}}^{(r)}}(t)\right)_{x_{\mathrm{i}}^{(r)}(t)}^{+} \\
&\quad+\sum_{l\in\mathcal{L}}\left(p_l(t)-\alpha_l^*\right)\left(z_l(t)-z_l^*\right) \\
&\le \sum_{f_{\mathrm{i}}\in\mathcal{F}_{\mathrm{i}}}\sum_{r=1}^{|\mathcal{R}_{\mathrm{i}}|}\left(x_{\mathrm{i}}^{(r)}(t)-x_{\mathrm{i}}^{*(r)}\right)\left(\bar{q}_{\mathrm{i}}(t)-q_{\mathbf{R}_{\mathrm{i}}^{(r)}}(t)\right) \\
&\quad+\sum_{l\in\mathcal{L}}\left(p_l(t)-\alpha_l^*\right)\left(z_l(t)-z_l^*\right) \\
&= \sum_{f_{\mathrm{i}}\in\mathcal{F}_{\mathrm{i}}}\sum_{r=1}^{|\mathcal{R}_{\mathrm{i}}|}\left(x_{\mathrm{i}}^{(r)}(t)-x_{\mathrm{i}}^{*(r)}\right)\left(\bar{q}_{\mathrm{i}}(t)-q_{\mathbf{R}_{\mathrm{i}}^{(r)}}(t)\right) \\
&\quad+\sum_{l\in\mathcal{L}}\left(p_l(t)-\alpha_l^*\right)\sum_{f_{\mathrm{i}}\in\mathcal{F}_{\mathrm{i}}}\sum_{r=1}^{|\mathcal{R}_{\mathrm{i}}|}\left(x_{\mathrm{i}}^{(r)}(t)-x_{\mathrm{i}}^{*(r)}\right)\mathbf{R}_{\mathrm{i}}^{(r)}[l] \\
&= \sum_{f_{\mathrm{i}}\in\mathcal{F}_{\mathrm{i}}}\sum_{r=1}^{|\mathcal{R}_{\mathrm{i}}|}\left(x_{\mathrm{i}}^{(r)}(t)-x_{\mathrm{i}}^{*(r)}\right)\left(\bar{q}_{\mathrm{i}}(t)-q_{\mathbf{R}_{\mathrm{i}}^{(r)}}(t)\right) \\
&\quad+\sum_{f_{\mathrm{i}}\in\mathcal{F}_{\mathrm{i}}}\sum_{r=1}^{|\mathcal{R}_{\mathrm{i}}|}\sum_{l\in\mathcal{L}}\left(p_l(t)-\alpha_l^*\right)\mathbf{R}_{\mathrm{i}}^{(r)}[l]\left(x_{\mathrm{i}}^{(r)}(t)-x_{\mathrm{i}}^{*(r)}\right) \\
&= \sum_{f_{\mathrm{i}}\in\mathcal{F}_{\mathrm{i}}}\sum_{r=1}^{|\mathcal{R}_{\mathrm{i}}|}\left(x_{\mathrm{i}}^{(r)}(t)-x_{\mathrm{i}}^{*(r)}\right)\left(\bar{q}_{\mathrm{i}}(t)-q_{\mathbf{R}_{\mathrm{i}}^{(r)}}(t)\right) \\
&\quad+\sum_{f_{\mathrm{i}}\in\mathcal{F}_{\mathrm{i}}}\sum_{r=1}^{|\mathcal{R}_{\mathrm{i}}|}\left(x_{\mathrm{i}}^{(r)}(t)-x_{\mathrm{i}}^{*(r)}\right)\left(q_{\mathbf{R}_{\mathrm{i}}^{(r)}}(t)-\beta_{\mathbf{R}_{\mathrm{i}}^{(r)}}^*\right) \\
&= \sum_{f_{\mathrm{i}}\in\mathcal{F}_{\mathrm{i}}}\sum_{r=1}^{|\mathcal{R}_{\mathrm{i}}|}\left(x_{\mathrm{i}}^{(r)}(t)-x_{\mathrm{i}}^{*(r)}\right)\left(\bar{q}_{\mathrm{i}}(t)-\beta_{\mathbf{R}_{\mathrm{i}}^{(r)}}^*\right) \\
&\le_{(a)} \sum_{f_{\mathrm{i}}\in\mathcal{F}_{\mathrm{i}}}\left(\left(\bar{q}_{\mathrm{i}}(t)-\beta_{\mathbf{R}_{\mathrm{i}}^{(1)}}^*\right)\sum_{r=1}^{|\mathcal{R}_{\mathrm{i}}|}\left(x_{\mathrm{i}}^{(r)}(t)-x_{\mathrm{i}}^{*(r)}\right)\right) \\
&=_{(b)} 0
\end{aligned} \tag{21}$$

where inequality (a) holds due to Lemma 1, and equality (b) holds due to the equality (10).

Thus, from inequalities (20) and (21), we can conclude that

$$\frac{d}{dt}V(\mathbf{p}(t),\mathbf{x}_{\mathrm{i}}(t))\le 0$$

for all t. Further more, from inequality (20), we also know that $\frac{d}{dt}V(\mathbf{p}(t),\mathbf{x}_{\mathrm{i}}(t))=0$ if and only if $\mathbf{x}_{\mathrm{e}}(t)=\mathbf{x}_{\mathrm{e}}^*$.

Appendix B
Proof of Proposition 5

We construct a partial Lagrangian to solve the FNO-DR problem. Let λ_l and μ_i^d be the Lagrange multipliers associated with the constraints (15) and (17), respectively. Furthermore, let $\boldsymbol{\lambda}=\{\lambda_l\}_l$ and $\boldsymbol{\mu}=\{\mu_i^d\}_{id}$ be the respective vectors; the partial Lagrangian can be written as

$$\begin{aligned}
L(\mathbf{x},\mathbf{r},\boldsymbol{\lambda},\boldsymbol{\mu}) &= \sum_{s,d\in\mathcal{N}}U_s^d\left(x_s^d\right)-\sum_{l\in\mathcal{L}}\lambda_l(y_l+z_l-c_l) \\
&\quad-\sum_{i,d\in\mathcal{N}}\mu_i^d\left(x_i^d+\sum_{m\in\mathcal{N}}r_{mi}^d-\sum_{j\in\mathcal{N}}r_{ij}^d\right)
\end{aligned}$$

IEEE Proof Print Version

$$= \sum_{s,d} \left(U_s^d(x_s^d) - \mu_s^d x_s^d\right) + \sum_d \left(\sum_{(i,j)\in\mathcal{L}} r_{ij}^d \left(\mu_i^d - \mu_j^d - \lambda_{ij}\right)\right) - \sum_l \lambda_l z_l + \sum_l \lambda_l c_l.$$

This problem satisfies Slater's condition, thus *strong duality* holds. From the optimality conditions, we know that the optimal solution $(\mathbf{x}^*, \mathbf{r}^*, \boldsymbol{\lambda}^*, \boldsymbol{\mu}^*)$ must satisfy the following conditions:

$$y_l^* + z_l^* \le c_l \qquad \forall\, l \in \mathcal{L} \tag{22}$$

$$x_i^{*d} + \sum_m r_{mi}^{*d} - \sum_j r_{ij}^{*d} \le 0 \qquad \forall\, i,d \in \mathcal{L} \tag{23}$$

$$x_s^{*d} = (U_s^d)'^{-1}\left(\mu_s^{*d}\right) \qquad \forall\, s,d \in \mathcal{N} \tag{24}$$

$$r_{ij}^{*d} \in, \arg\max_{0\le r_{ij}^d \le P} \sum_d \left(\sum_{(i,j)\in\mathcal{L}} r_{ij}^d \left(\mu_i^{*d} - \mu_j^{*d} - \lambda_{ij}^*\right)\right) \tag{25}$$

$$\lambda_l^* \left(y_l^* + z_l^* - c_l^*\right) = 0 \qquad \forall\, l \in \mathcal{L} \tag{26}$$

$$\mu_i^{*d}\left(x_i^{*d} + \sum_{m\in\mathcal{N}} r_{mi}^{*d} - \sum_{j\in\mathcal{N}} r_{ij}^{*d}\right) = 0 \qquad \forall\, i,d \in \mathcal{N} \tag{27}$$

where (22) and (23) are the primal feasibility, (24) and (25) are the primal optimality condition, and (25)–(27)***[(25) is mentioned twice. Is this correct?]*** are the complementary slackness condition.

Define a Lyapunov function

$$V(\mathbf{p}(t),\mathbf{s}(t),\mathbf{x}_i(t),\mathbf{r}(t)) = \frac{1}{2}\sum_{l\in\mathcal{L}} \left(p_l(t) - \lambda_l^*\right)^2 + \frac{1}{2}\sum_{f_i\in\mathcal{F}_i}\sum_{r=1}^{|\mathcal{R}_i|}\left(x_i^{(r)}(t) - x_i^{*(r)}\right)^2 + \frac{1}{2}\sum_{i,d\in\mathcal{N}}\left(s_i^d(t) - \mu_i^{*d}\right)^2 + \frac{1}{2}\sum_{(i,j)\in\mathcal{L},d\in\mathcal{N}}\left(r_{ij}^d(t) - r_{ij}^{*d}\right)^2.$$

Then, its drift is given by the following (from here, we omit the time index (t) for brevity):

$$\frac{d}{dt}V(\mathbf{p},\mathbf{s},\mathbf{x}_i,\mathbf{r}) = \sum_l \left(p_l - \lambda_l^*\right)\left(z_l + y_l - c_l\right)_{p_l}^+ + \sum_{f_i\in\mathcal{F}_i}\sum_{r=1}^{|\mathcal{R}_i|}\left(x_i^{(r)} - x_i^{*(r)}\right) \times \left(\bar{q}_i - q_{\mathbf{R}_i^{(r)}}\right)_{x_i^{(r)}}^+ + \sum_{i,d}\left(s_i^d - \mu_i^{*d}\right) \times \left(x_i^d + \sum_m r_{mi}^d - \sum_j r_{ij}^d\right)_{s_i^d}^+ + \sum_{(i,j),d}\left(r_{ij}^d - r_{ij}^{*d}\right)\dot{r}_{ij}^d$$

$$\le \sum_{l\in\mathcal{L}}\left(p_l - \lambda_l^*\right)\left(z_l - z_l^*\right) \tag{28}$$

$$+ \sum_{l\in\mathcal{L}}\left(p_l - \lambda_l^*\right)\left(y_l + z_l^* - c_l\right) \tag{29}$$

$$+ \sum_{f_i\in\mathcal{F}_i}\sum_{r=1}^{|\mathcal{R}_i|}\left(x_i^{(r)} - x_i^{*(r)}\right) \times \left(\bar{q}_i - q_{\mathbf{R}_i^{(r)}}\right) \tag{30}$$

$$+ \sum_{i,d}\left(s_i^d - \mu_i^{*d}\right) \times \left(x_i^d + \sum_m r_{mi}^d - \sum_j r_{ij}^d\right) \tag{31}$$

$$+ \sum_{(i,j),d}\left(r_{ij}^d - r_{ij}^{*d}\right)\left(s_i^d - s_j^d - p_{ij}\right). \tag{32}$$

Next, we show the negativity of the drift. First, from the proof of the fixed route scenario, we know that $(28)+(30) \le 0$ follows the same reasoning there

$$(29)+(30) \le \sum_{(i,j)\in\mathcal{L}}\left(p_{ij} - \lambda_{ij}^*\right)\left(\sum_d r_{ij}^d - \sum_d r_{ij}^{*d}\right) + \sum_{i,d}\left(s_i^d - \mu_i^{*d}\right)\left(x_i^d + \sum_m r_{mi}^d - \sum_j r_{ij}^d\right)$$

$$= \sum_{(i,j)\in\mathcal{L}}\left(p_{ij} - \lambda_{ij}^*\right)\left(\sum_d r_{ij}^d - \sum_d r_{ij}^{*d}\right) \tag{33}$$

$$+ \sum_{i,d}\left(s_i^d - \mu_i^{*d}\right)\left(x_i^d - x_i^{*d}\right) \tag{34}$$

$$+ \sum_{i,d}\left(s_i^d - \mu_i^{*d}\right)\left(x_i^{*d} + \sum_m r_{mi}^d - \sum_j r_{ij}^d\right). \tag{35}$$

Notice that

$$(34) = \sum_{i,d}\left(\left(U_s^d\right)'\left(x_i^d\right) - \left(U_s^d\right)'\left(x_i^{*d}\right)\right)\left(x_i^d - x_i^{*d}\right)$$

and the assumption that the utility function U_s^d is a concave function, we have $(37) \le 0$. By adding and subtracting the same term $\sum_{i,d}\left(\mu_i^{*d}\left(\sum_m r_{mi}^{*d} - \sum_j r_{ij}^{*d}\right)\right)$ to the rest of the terms, we get

$$(33)+(35) = \sum_{(i,j),d} p_{ij} r_{ij}^d - \sum_{(i,j),d} p_{ij} r_{ij}^{*d} - \sum_{(i,j),d}\lambda_{ij}^* r_{ij}^d \tag{36}$$

$$+ \sum_{(i,j),d}\lambda_{ij}^* r_{ij}^{*d} \tag{37}$$

$$+ \sum_{i,d}\left(x_i^{*d} s_i^d + s_i^d\left(\sum_m r_{mi}^d - \sum_j r_{ij}^d\right)\right) \tag{38}$$

IEEE Proof Print version

$$-\sum_{i,d}\left(x_i^{*d}\mu_i^{*d}+\mu_i^{*d}\left(\sum_m r_{mi}^{*d}-\sum_j r_{ij}^{*d}\right)\right) \quad (39)$$

$$+\sum_{i,d}\left(\mu_i^{*d}\left(\sum_m r_{mi}^{*d}-\sum_j r_{ij}^{*d}\right)\right) \quad (40)$$

$$-\sum_{i,d}\left(\mu_i^{*d}\left(\sum_m r_{mi}^{d}-\sum_j r_{ij}^{d}\right)\right). \quad (41)$$

Note that $(39)=0$ by (27). Combine the first term in (36) with (38), the third term with (41) and (37) with (40), and we get

$$\begin{aligned}
(33)+(35)=&-\sum_{(i,j),d} p_{ij}r_{ij}^{*d}\\
&+\left(\sum_{i,d}x_i^{*d}s_i^d-\sum_{(i,j),d}r_{ij}^d\left(s_i^d-s_j^d-p_{ij}\right)\right)\\
&-\left(\sum_{(i,j),d}r_{ij}^{*d}\left(\mu_i^{*d}-\mu_j^{*d}-\lambda_{ij}^*\right)\right)\\
&+\left(\sum_{(i,j),d}r_{ij}^{d}\left(\mu_i^{*d}-\mu_j^{*d}-\lambda_{ij}^*\right)\right)\\
\le_{(a)}&-\sum_{(i,j),d} p_{ij}r_{ij}^{*d}\\
&+\left(\sum_{i,d}x_i^{*d}s_i^d-\sum_{(i,j),d}r_{ij}^d\right.\\
&\qquad\left.\times\left(s_i^d-s_j^d-p_{ij}\right)\right)\\
\le_{(b)}&\sum_{i,d}\left(\sum_j r_{ij}^{*d}-\sum_m r_{mi}^{*d}\right)s_i^d\\
&-\sum_{(i,j),d}p_{ij}r_{ij}^{*d}-\sum_{(i,j),d}r_{ij}^d\\
&\qquad\times\left(s_i^d-s_j^d-p_{ij}\right)\\
=&\sum_{(i,j),d}r_{ij}^{*d}\left(s_i^d-s_j^d-p_{ij}\right)\\
&-\sum_{(i,j),d}r_{ij}^d\left(s_i^d-s_j^d-p_{ij}\right)\\
=&-(32)
\end{aligned}$$

where (a) holds since r_{ij}^{*d} maximizes $\sum_{(i,j),d}r_{ij}^d\left(\mu_i^{*d}-\mu_j^{*d}-\lambda_{ij}^*\right)$ over all r_{ij}^d, thus $\sum_{(i,j),d}r_{ij}^{*d}\left(\mu_i^{*d}-\mu_j^{*d}-\lambda_{ij}^*\right)\ge\sum_{(i,j),d}r_{ij}^{d}\left(\mu_i^{*d}-\mu_j^{*d}-\lambda_{ij}^*\right)$ and (b) holds follow from (23).

Thus, we conclude that

$$\frac{d}{dt}V(\mathbf{p}(t),\mathbf{s}(t),\mathbf{x_i}(t),\mathbf{r}(t))\le 0$$

for all t, and the equality holds if and only if $\mathbf{x}_e(t)=\mathbf{x}_e^*$.

REFERENCES

[1] E. Altman, T. Başar, and R. Srikant, "Congestion control as a stochastic control problem with action delays," *Automatica*, vol. 35, pp. 1937–1950, 1999.

[2] J. Bolot and A. Shankar, "Dynamic behavior of rate-based flow cntrol mechanisms," *ACM Comput. Commun. Rev.*, vol. 20, no. 2, 1992***[Pages?]***.

[3] S. Borst and N. Hegde, "Integration of streaming and elastic traffic in wireless networks," in *Proc. IEEE INFOCOM*, May 2007, pp. 1884–1892.

[4] S. Boyd and L. Vandenberghe, *Convex Optimization*. Cambridge, U.K.: Cambridge Univ. Press, 2004.

[5] L. Bui, A. Eryilmaz, R. Srikant, and X. Wu, "Joint asynchronous congestion control and distributed scheduling for wireless networks," in *Proc. IEEE INFOCOM*, 2006.

[6] A. Eryilmaz and R. Srikant, "Fair resource allocation in wireless networks using queue-length based scheduling and congestion control," in *Proc. IEEE INFOCOM*, Miami, FL, Mar. 2005, vol. 3, pp. 1794–1803.

[7] A. Eryilmaz and R. Srikant, "Resource allocation of multi-hop wireless networks," in *Proc. Int. Zurich Seminar Commun.*, Feb. 2006***[Pages?]***.

[8] A. Eryilmaz, R. Srikant, and J. R. Perkins, "Stable scheduling policies for fading wireless channels," *IEEE/ACM Trans. Networking*, vol. 13, no. 2, pp. 411–425, Apr. 2005.

[9] L. Georgiadis, M. J. Neely, and L. Tassiulas, *Resource Allocation and Cross-Layer Control in Wireless Networks*, ser. Foundations and Trends in Networking. Hanover, MA: now, 2006.

[10] P. Hande, S. Zhang, and M. Chiang, "Distributed rate allocation for inelastic flows," *IEEE/ACM Trans. Netw.*, vol. 15, no. 6, pp. 1240–1253, Dec. 2007.

[11] K. Kar, S. Sarkar, and L. Tassiulas, "A simple rate control algorithm for maximizing total user utillity," in *Proc. IEEE INFOCOM*, Anchorage, AK, 2001, vol. 1, pp. 133–141.

[12] F. P. Kelly, A. Maulloo, and D. Tan, "Rate control in communication networks: Shadow prices, proportional fairness and stability," *J. Oper. Res. Soc.*, vol. 49, pp. 237–252, 1998.

[13] S. Kunniyur and R. Srikant, "An adaptive virtual queue (AVQ) algorithm for active queue management," *IEEE/ACM Trans. Netw.*, vol. 12, no. 2, pp. 286–299, Apr. 2004.

[14] J. Lee, R. R. Mazumdar, and N. Shroff, "Non-convex optimization and rate control for multi-class services in the internet," *IEEE/ACM Trans. Netw.*, vol. 13, no. 4, pp. 827–840, Aug. 2005.

[15] R. Li, A. Eryilmaz, L. Ying, and N. B. Shroff, "A unified approach to optimizing performance in networks serving heterogeneous flows," in *Proc. IEEE INFOCOM*, 2009, pp. 253–261.

[16] X. Lin and N. Shroff, "Joint rate control and scheduling in multihop wireless networks," in *Proc. IEEE CDC*, Paradise Island, Bahamas, Dec. 2004, vol. 2, pp. 1484–1489.

[17] X. Lin and N. Shroff, "The impact of imperfect scheduling on cross-layer rate control in multihop wireless networks," in *Proc. IEEE INFOCOM*, Miami, FL, Mar. 2005, vol. 3, pp. 1804–1814.

[18] X. Lin, N. B. Shroff, and R. Srikant, "A tutorial on cross-layer optimization in wireless networks," *IEEE J. Sel. Areas Commun.*, vol. 24, no. 8, pp. 1452–1463, Aug. 2006.

[19] S. H. Low and D. E. Lapsley, "Optimization flow control, I: Basic algorithm and convergence," *IEEE/ACM Trans. Netw.*, vol. 7, no. 6, pp. 861–875, Dec. 1999.

[20] E. Mallada and F. Paganini, "Stability of node-based multipath routing and dual congestion control," in *Proc. 47th IEEE CDC*, Dec. 2008, pp. 1398–1403.

[21] M. Neely, E. Modiano, and C. Li, "Fairness and optimal stochastic control for heterogeneous networks," in *Proc. IEEE INFOCOM*, Miami, FL, Mar. 2005, pp. 1723–1734.

[22] M. Neely, E. Modiano, and C. Rohrs, "Dynamic power allocation and routing for time varying wireless networks," in *Proc. IEEE INFOCOM*, Apr. 2003, pp. 745–755.

[23] S. Patil and G. Veciana, "Managing resources and quality of service in heterogeneous wireless systems exploiting opportunism," *IEEE/ACM Trans. Netw.*, vol. 15, no. 5, pp. 1046–1058, Oct. 2007.

[24] D. Qiu and N. B. Shroff, "A predictive flow control scheme for efficient network utilization and QoS," *IEEE/ACM Trans. Netw.*, vol. 12, no. 1, pp. 161–172, Feb. 2004.

[25] S. Shakkottai and A. Stolyar, "Scheduling algorithms for a mixture of real-time and non-real-time data in hdr," in *Proc. 17th ITC*, 2001, pp. 793–804.

IEEE Proof Print Version

[26] R. Srikant, *The Mathematics of Internet Congestion Control*. Boston, MA: Birkhäuser, 2004.
[27] A. Stolyar, "Maximizing queueing network utility subject to stability: Greedy primal-dual algorithm," *Queue. Syst.*, vol. 50, no. 4, pp. 401–457, 2005.
[28] L. Tassiulas and A. Ephremides, "Stability properties of constrained queueing systems and scheduling policies for maximum throughput in multihop radio networks," *IEEE Trans. Autom. Control*, vol. 36, no. 12, pp. 1936–1948, Dec. 1992.
[29] X. Wu and R. Srikant, "Regulated maximal matching: A distributed scheduling algorithm for multi-hop wireless networks with node-exclusive spectrum sharing," in *Proc. IEEE CDC*, 2005, pp. 5342–5347.
[30] L. Ying, R. Srikant, A. Eryilmaz, and G. E. Dullerud, "Distributed fair resource allocation in cellular networks in the presence of heterogeneous delays," in *Proc. WiOPT*, 2005, pp. 96–105.

Ruogu Li (S'10) received the B.S. degree in electronic engineering from Tsinghua University, Beijing, China, in 2007, and is currently pursuing the Ph.D. degree in electrical and computer engineering at the Ohio State University, Columbus.

His research interests include optimal network control, wireless communication networks, low-delay scheduling scheme design, and cross-layer algorithm design.

Atilla Eryilmaz (S'00–M'06) received the M.S. and Ph.D. degrees in electrical and computer engineering from the University of Illinois at Urbana-Champaign in 2001 and 2005, respectively.

Between 2005 and 2007, he worked as a Post-Doctoral Associate with the Laboratory for Information and Decision Systems, Massachusetts Institute of Technology, Cambridge. He is currently an Assistant Professor of electrical and computer engineering with the Ohio State University, Columbus. His research interests include communication networks, optimal control of stochastic networks, optimization theory, distributed algorithms, stochastic processes, and network coding.

Dr. Eryilmaz received the National Science Foundation CAREER Award in 2010.

Lei Ying (M'07) received the B.E. degree from Tsinghua University, Beijing, China, in 2001, and the M.S. and Ph.D. degrees in electrical engineering from the University of Illinois at Urbana-Champaign in 2003 and 2007, respectively.

During Fall 2007, he worked as a Post-Doctoral Fellow with the University of Texas at Austin. He is currently an Assistant Professor with the Department of Electrical and Computer Engineering, Iowa State University, Ames, where he is named the Litton Assistant Professor for 2010–2011. His research interest is broadly in the area of information networks, including wireless networks, mobile ad hoc networks, P2P networks, and social networks.

Dr. Ying received a Young Investigator Award from the Defense Thread Reduction Agency (DTRA) in 2009, and a National Science Foundation CAREER Award in 2010.

Ness B. Shroff (S'91–M'93–SM'01–F'07) received the Ph.D. degree from Columbia University, New York, NY, in 1994.

He is currently the Ohio Eminent Scholar of Networking and Communications and a Professor of electrical and computer engineering (ECE) and computer science and engineering with the Ohio State University, Columbus. He also currently serves as a Guest Chaired Professor of wireless communications with the Department of Electronic Engineering, Tsighnua University, Beijing, China. Previously, he was a Professor of ECE with Purdue University, West Lafayette, IN, and the Director of the Center for Wireless Systems and Applications (CWSA), a university-wide center on wireless systems and applications. His research interests span the areas of wireless and wireline communication networks, where he investigates fundamental problems in the design, performance, pricing, and security of these networks.

Dr. Shroff has received numerous awards for his networking research, including the National Science Foundation CAREER award, the Best Paper awards for IEEE INFOCOM 2006 and 2008, the Best Paper Award for IEEE IWQoS 2006, the Best Paper of the Year Award for *Computer Networks*, and the Best Paper of the Year Award for the *Journal of Communications and Networks* (his IEEE INFOCOM 2005 paper was one of two runner-up papers).

IEEE Proof
Print Version